neous cpm)] × 100. Spontaneous and maximal release cpm were determined by incubating $1 \times 10^4$ PR8-infected and $^{51}$C-labeled P815 cells with 100 μl of a medium and 100 μl of 5% Triton X-100, respectively.

### 2.13. Statistical analyses

Differences in virus titers of groups between the wild-type and pIgR-deficient mice were compared by ANOVA. Comparisons between experimental groups were performed by Student's *t*-test. $P < 0.05$ was considered significant unless otherwise indicated.

## 3. Results

### 3.1. Protection against influenza virus infection in BALB/c mice immunized intranasally with CT112K-combined vaccine

The effectiveness of CT112K as an adjuvant of the nasal influenza vaccine on the protection against influenza virus infection was investigated in BALB/c mice. The mice received a primary intranasal administration of the CT112K (0.1 μg)-combined PR8 vaccine (0.1 μg) and a second intranasal administration of the PR8 vaccine (0.1 μg) with or without CT112K 4 weeks later. Two weeks after the second immunization, the mice were challenged with either a nonlethal dose (2 μl) or a lethal dose (20 μl) of the suspension of PR8 viruses. Three days after the challenge, nasal wash virus titers in mice challenged with a nonlethal dose of the viruses and lung wash virus titers in mice challenged with a lethal dose of the viruses were determined as the indexes of protection in the upper RT and in the lower RT, respectively. Fig. 1 shows that based on the nasal and lung wash virus titers 3 days after infection, the two-dose regimen, which is composed of primary immunization with the CT112K (0.1 μg)-combined PR8 vaccine (0.1 μg) and the secondary immunization with the PR8 vaccine (0.1 μg) with or without CT112K 4 weeks later, conferred complete protection against infection in either the upper RT or the lower RT. The primary immunization with the CT112K-combined vaccine alone conferred complete protection against infection in the upper RT but only partial protection against infection in the lower RT. The primary and the secondary immunizations with the vaccine alone in control mice, and the vaccine alone at the time of secondary administration conferred no protection. Thus, the protection induced by the primary immunization alone was less than that induced by the second immunization. This finding suggests that the degree of protection depends on the magnitude of the immune responses.

Kinetics of nasal wash and lung wash virus titers 1–3 days after challenge infection were also examined in mice challenged with a lethal dose of the viruses, to determine the onset of virus elimination. Fig. 2 shows that nasal and lung wash virus titers were not detected from day 1 post-infection in mice immunized by the two-dose regimen. Thus, the protection against infection in the immunized mice was probably initiated immediately after the challenge virus infection.

From the standpoint of safety of vaccination, the use of the vaccine alone as the secondary antigen in mice immunized primarily with the CT112K-combined vaccine 4 weeks pre-

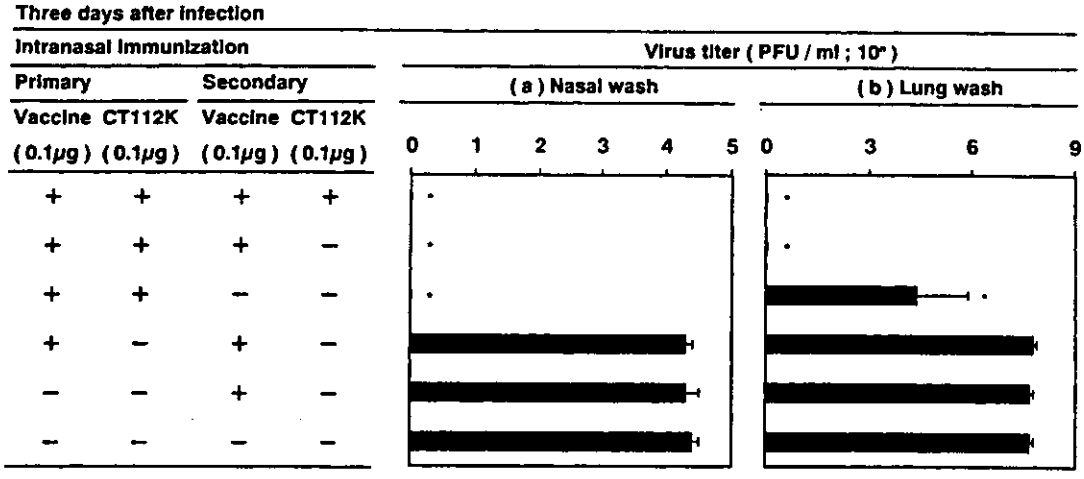


Fig. 1. Protection against PR8 virus infection in mice that received a primary intranasal administration of CT112K-combined PR8 vaccine and a secondary intranasal administration of the vaccine alone 4 weeks later. Two weeks after the second vaccination, mice were challenged with either a nonlethal dose of PR8 viruses (the upper RT infection) (a) or a lethal dose of PR8 viruses (the total RT infection) (b). Three days after infection, nasal wash virus titer (PFU/ml) in mice with the upper RT infection and lung wash virus titer (PFU/ml) in mice with the total RT infection were determined as an index of protection. Each bar represents the mean virus titer ± S.D. of each group of five mice. Mice with virus titers below the limit of detection (less than 5 PFU/ml) were considered to have cleared the infection, and the value 0 was assigned for the purpose of statistical analysis. Asterisk indicates significant difference from nonimmunized control mice ($P < 0.05$) in mean nasal wash and lung wash virus titers.

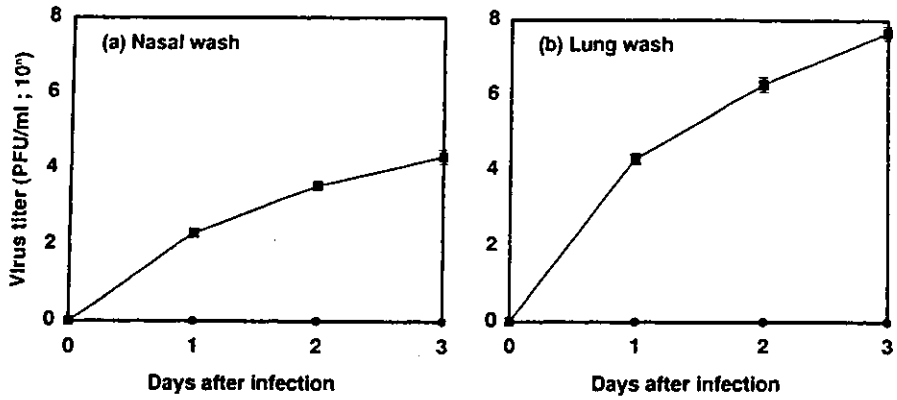


Fig. 2. Kinetics of nasal wash (a) and lung wash (b) virus titers 1–3 days after challenge infection in mice challenged with a lethal dose of the viruses. For other details, see Fig. 1.

viously will be better than the use of the CT112K-combined vaccine. In addition, both 0.1 μg of CT112K and 0.1 μg of vaccine for the primary immunization and 0.1 μg of vaccine for the second immunization seem to be close to the minimal effective dose for providing complete protection against infection with a lethal dose of viruses. In the subsequent experiments, Ab and T cell-mediated immune responses to the two-dose regimen were characterized in mice.

### 3.2. AFC and Ab responses in mice immunized by the two-dose regimen

IgA, IgG and IgM AFC responses to PR8 vaccines in the NALT and the spleen were investigated in mice immunized primarily with the CT112K (0.1 μg)-combined PR8 vaccine (0.1 μg) and secondarily with the PR8 vaccine (0.1 μg) 4 weeks later. Fig. 3A shows that in the NALT, only low levels

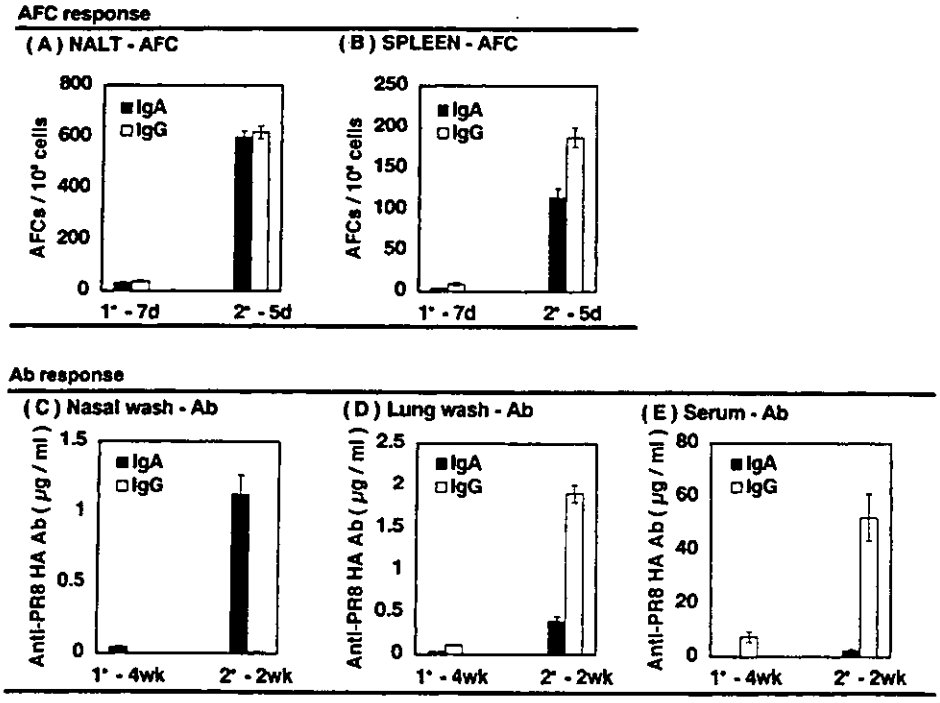


Fig. 3. IgA and IgG AFC responses in the NALT (A) and spleen (B) 7 days after primary (1°) vaccination and 5 days after secondary (2°) vaccination in mice that received a primary intranasal administration of CT112K-combined PR8 vaccine and a secondary intranasal administration of the vaccine alone 4 weeks later are shown. Each column represents the mean AFC/$10^6$ cells ± S.D. in duplicate ELISPOT assays of pooled cell suspension from each group of five mice. IgA and IgG Ab titers in the nasal wash (C), lung wash (D) and serum (E) 4 weeks after primary (1°) vaccination and 2 weeks after secondary (2°) vaccination in the two-dose regimen are also shown. Each column represents the mean Ab titer ± S.D. in each group of five mice.

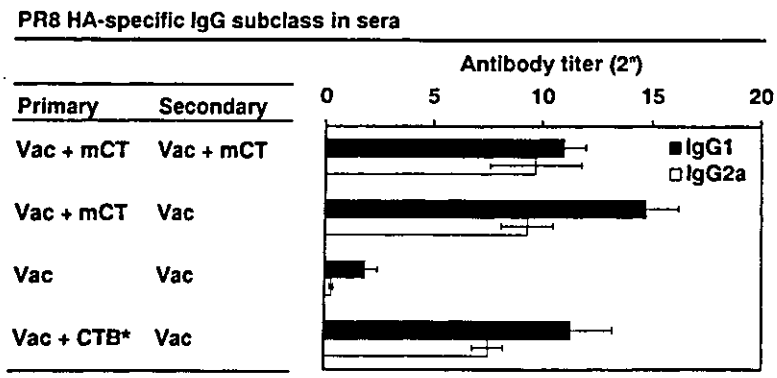


Fig. 4. PR8 HA-specific IgG subclass Ab titers in the sera of mice that received a primary intranasal administration of CT112K-combined PR8 vaccine and a secondary intranasal administration of the vaccine alone 4 weeks later. Each bar represents the mean Ab titer ± S.D. in each group of five mice.

of IgA and IgG AFC responses were detected 7 days after the primary immunization, while high levels of IgA and, IgG AFC responses were detected 5 days after the second immunization. Fig. 3B shows that in the spleen, only low levels of the IgG AFC response were detected 7 days after the primary immunization, while high levels of IgG and IgA-AFC responses were detected 5 days after the second immunization.

Ab responses to PR8 HA molecules in the nasal wash based on the Ab titers, lung wash and serum were also examined 4 weeks after the primary immunization and 2 weeks after the second immunization. Fig. 3C shows that high levels of IgA Abs, which were much higher than the IgG levels, were detected in the nasal wash 2 weeks after the second immunization, although low levels of IgA and IgG Ab responses were detected 4 weeks after the primary immunization. Thus, with respect to the IgA and IgG Ab responses, the segregation between the AFC responses in the NALT (Fig 3A) and the Ab responses in the nasal wash (Fig. 3C) was observed. Fig. 3D shows that the secondary-type IgG Ab responses, whose levels were higher than those of the IgA Ab responses, were detected in the lung wash 2 weeks after the second immunization. The secondary-type IgG Ab responses, whose levels were higher than those of the IgA responses, were also detected in the serum 2 weeks after the second immunization (Fig. 3E).

The titers of subclasses of anti-HA IgG Abs were also examined in the serum from mice 2 weeks after the second immunization. Fig. 4 shows that high levels of both IgG1 and IgG2a, in which the IgG1 level is significantly higher than the IgG2a level, were observed.

These results suggest that in the nasal wash, a low but appreciable level of IgA Ab 4 weeks after the primary immunization and a high level of IgA Ab 2 weeks after the second immunization correlate with the complete protection against virus infection in the upper RT (Figs. 1 and 2). These also suggest that in the lung wash, a low level of IgG Ab 4 weeks after the primary immunization and a high level of IgG Ab 2 weeks after the secondary immunization correlate with the partial and the complete protection in the lower RT, respectively (Figs. 1 and 2).

### 3.3. Memory DTH responses in mice immunized by the two-dose regimen

DTH responses to PR8 vaccines were examined in mice immunized by the two-dose regimen. On various days after the primary and secondary immunizations, the DTH-eliciting antigen (PR8 vaccine) was injected into the footpads and 24 h later, footpad swelling was determined as an index of DTH. Fig. 5 shows that the group of mice immunized by the two-dose regimen exhibited the DTH response that started from 5 days, peaked 7 days and decreased 28 days after the primary immunization. The second immu-

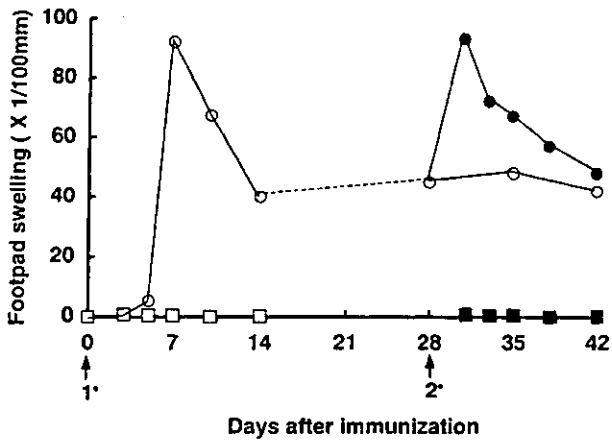


Fig. 5. Kinetics of DTH response to PR8 vaccine in mice that received a primary intranasal administration of CT112K-combined PR8 vaccine and a secondary intranasal administration of the vaccine alone 4 weeks later (●). The DTH response of mice that received only the primary CT112K-combined PR8 vaccine (○) or that of mice that received only the primary PR8 vaccine (□) or both primary and secondary PR8 vaccines (■) is also shown. Each point is the mean footpad swelling ± S.D. in each group of five mice.

nization administered 28 days (4 weeks) after the primary immunization induced an accelerated DTH response which was detected 3 days after the second immunization and accompanied by the same peak height as that in the case of the primary DTH response. In addition, the magnitude of DTH response 2 weeks after the second immunization was relatively low and corresponded to the magnitude 4 weeks after the primary immunization. These results suggest that the memory DTH response is not mainly involved in the protection that depends on the magnitude of immune responses and is provided by an immediate effect of preventing infection 2 weeks after the secondary immunization (Figs. 1 and 2).

### *3.4. CTL memory cell responses in mice immunized by the two-dose regimen*

CTL activities against PR8 virus-infected cells were examined in mice immunized by the two-dose regimen. The spleen cells from mice 2 weeks after the secondary immunization showed no CTL activity, as directly determined by a $^{51}Cr$ release assay of PR8 virus-infected P815 cells. The spleen cells were then cultured in vitro for 5 days with stimulator cells, which were autologous spleen cells infected with the PR8 virus. As controls, spleen cells from either mice infected intranasally with a nonlethal dose of a PR8 virus suspension ($10^{4.1}$ $EID_{50}$, 1 μl of the virus suspension into each nostril) 2 weeks previously, from mice that received both the primary and secondary immunizations with the vaccine alone, or from naive mice were cultured. Fig. 6 shows that 5 days after culture, spleen cells

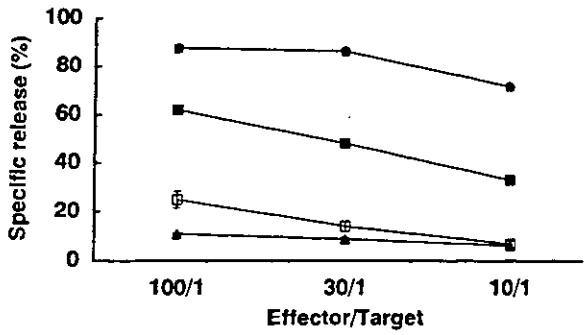


Fig. 6. Memory CTL activity in mice that received a primary intranasal administration of CT112K-combined PR8 vaccine and a secondary intranasal administration of the vaccine alone 4 weeks later. Spleen cells from mice immunized by the two-dose regimen were co-cultured with PR8 virus-infected autologous spleen cells for 5 days. The memory CTL activity was assayed based on the amount of $^{51}Cr$ released against PR8 virus-infected P815 target cells. The memory CTL activities of spleen cells from mice infected with a small volume of virus suspension 2 weeks previously (●), from mice that received a primary CT112K-combined PR8 vaccine and a secondary PR8 vaccine alone 4 weeks later (■), from mice that received both primary and secondary PR8 vaccine alone (□), and from nonimmunized mice (▲) are shown in the figure. Each point represents the mean ± S.D. of triplicate samples from pooled spleen cells in each group of five mice.

from mice immunized by the two-dose regimen exhibited CTL responses which were stronger than those of the cells from mice given two doses of the vaccine alone and from naive mice, but weaker than those of the cells derived from infected mice. Thus, the relatively high CTL memory cell activity was generated by the 5-day culture of spleen cells from the mice immunized by the two-dose regimen, although it was lower than those of the cells from the infected mice. The data indicating that a few days are required for the generation of the CTL activity in vitro suggest that the CTL activity is not mainly involved in the protection, which is provided by an immediate effect of preventing infection 2 weeks after the secondary immunization (Fig. 2).

### *3.5. Ab responses and cross-protection in mice immunized by the two-dose regimen*

The data presented above suggest that in the nasal wash, a low but appreciable level of IgA Ab 4 weeks after the primary immunization and a high level of IgA Ab 2 weeks after the secondary immunization correlate with the complete protection against the virus infection in the upper RT, while in the lung wash, a low level of IgG Abs 4 weeks after the primary immunization and a high level of the IgG Abs 2 weeks after the secondary immunization correlate with the partial and complete protections in the lower RT (Fig. 1). To clarify the significance of these data, mice were given the primary immunization with different CT112K-combined vaccines, which were prepared from PR8 (H1N1), A/Beijing (H1N1), A/Yamagata (H1N1), A/Guizhou (H3N2) and B/Ibaraki viruses, and the secondary immunization with the respective vaccines without CT112K 4 weeks later. Two weeks after the secondary immunization, mice were challenged with either a nonlethal (2 μl) or a lethal dose (20 μl) of a suspension of the PR8 virus. Three days after the challenge, the nasal wash virus titers in mice challenged with a nonlethal dose of the virus and the lung wash virus titers in mice challenged with a lethal dose of the virus were determined. Fig. 7A shows the PR8 HA-reactive IgA Ab and virus titers in the nasal wash of the various groups of mice immunized by the two-dose regimen. The immunization with the PR8 (H1N1) vaccine conferred complete protection against the PR8 virus infection and was accompanied by a predominantly high PR8 HA-reactive IgA Ab titer in the nasal wash. The immunization with A/Beijing (H1N1) or the A/Yamagata (H1N1) vaccine conferred complete or partial cross-protection against the PR8 virus challenge, and was accompanied by a relatively high PR8 HA-reactive IgA Ab titer in the nasal wash. The A/Guizhou (H3N2) vaccine also provided a low level of protection with a low PR8 HA-reactive IgA Ab titer. The B/Ibaraki vaccine provided a marginal level of protection with almost no induction of Ab responses, compared with the nonimmunized control. In this regard, we have previously shown that influenza-type nonspecific mechanisms may often be involved in this type of immunization [5]. Thus, in the nasal wash, the protection

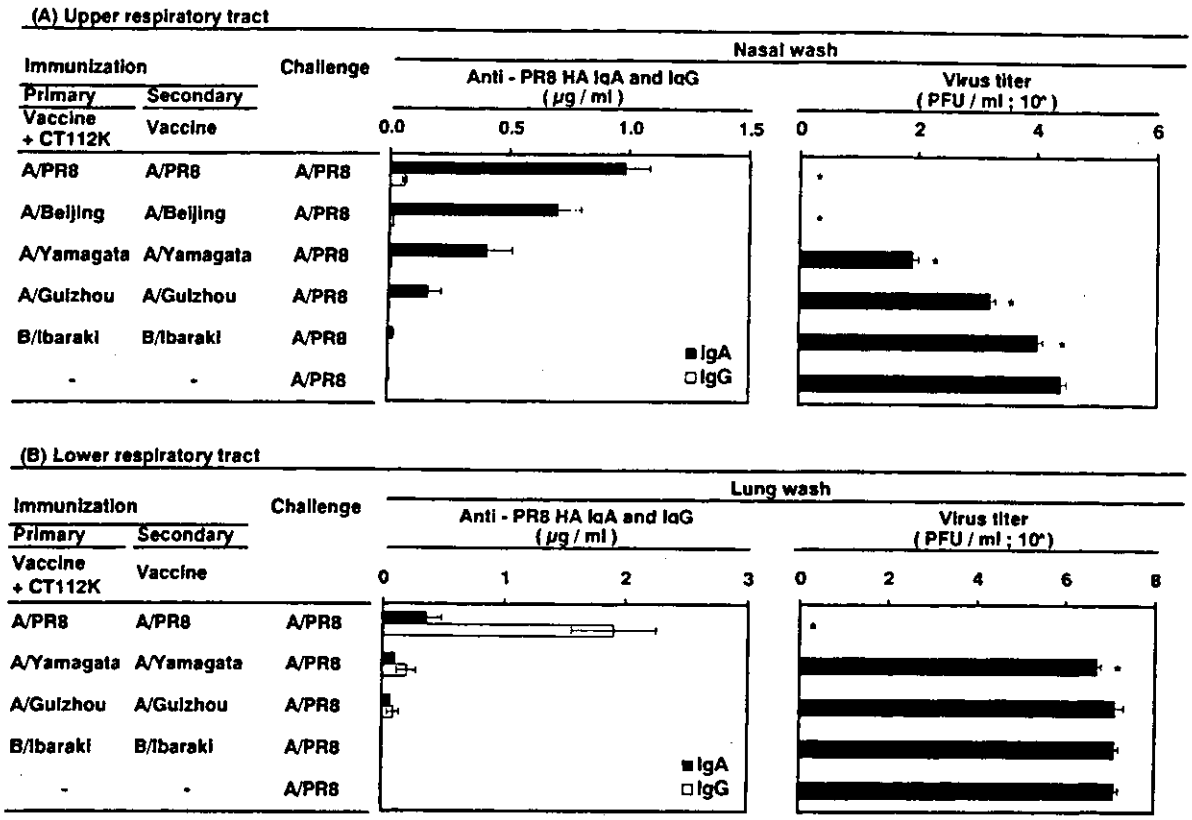


Fig. 7. PR8 HA-reactive Ab responses and protection against influenza virus infection in mice that received a primary intranasal administration of CT112K-combined with different inactivated vaccines that were prepared from A/PR8 (H1N1), A/Beijing (H1N1), A/Yamagata (H1N1), A/Guizhou (H3N2) and B/Ibaraki viruses, and a secondary intranasal administration of the respective vaccines 4 weeks later. Two weeks after the secondary immunization, mice were challenged by either an upper RT infection (A) or a total RT infection (B). Three days after the challenge, nasal wash specimens from mice challenged by an upper RT infection (A) or lung wash specimens from mice challenged by a total RT infection (B) were obtained for anti-PR8 HA IgA and IgG Ab titration and for virus titration. Each bar represents the mean PR8 HA-reactive or IgG titer ± S.D. in nasal and lung washes or the mean virus titers ± S.D. in nasal and lung washes. Mice with virus titers below the limit of detection (less than 5 PFU/ml) were considered to have cleared the infection, and the value 0 was assigned for the purpose of statistical analysis. Asterisk indicates significant difference from nonimmunized control mice ($P < 0.05$) in mean nasal wash and lung wash virus titers.

or cross-protection against the upper RT infection was accompanied by the predominant induction of the IgA Ab response, which are cross-reactive to PR8 HA.

Fig. 7B shows PR8 HA-reactive IgA Abs and virus titers in the lung wash of the various groups of mice immunized by the two-dose regimen. The immunization with the PR8 (H1N1) vaccine conferred complete protection against the PR8 virus infection and was accompanied by a predominantly high PR8 HA-reactive IgG Ab titer in the lung wash. The immunization with the A/Beijing (H1N1) vaccine conferred partial cross-protection against the PR8 virus challenge, and was accompanied by a low PR8 HA-reactive IgA Ab titer in the lung wash. The A/Yamagata (H1N1), the A/Guizhou (H3N2) or B/Ibaraki vaccine provided no cross-protection with almost no induction of Ab responses. Thus, in the lung wash, the protection or cross-protection against the lower RT infection was accompanied by the predominant induction of the IgG Ab response, which are less cross-reactive to PR8 HA than the IgA Abs.

## 4. Discussion

In the present paper, immune responses induced by the nasal CT112K-combined influenza vaccine were characterized in BALB/c mice, which received a primary administration of the adjuvant (0.1 μg)-combined PR8 vaccine (0.1 μg) and the secondary administration of the vaccine alone (0.1 μg) 4 weeks later. The two-dose regimen conferred complete protection against infection, although the primary immunization alone conferred only partial protection (Fig. 1). In addition, the protection against infection in the immunized mice was initiated immediately after the challenge infection (Fig. 2). Enhanced IgA, IgG and IgM AFC responses, compared with the primary responses, were induced in the NALT and the spleen (Fig. 3). The presence of IgA-AFC responses in the spleen may be explained by IgA-AFCs trapped by spleen on the way to home mucosal-associated tissues. In parallel with the AFC responses, higher levels of nasal wash, lung wash and

serum anti-PR8 HA IgA and IgG Ab responses than the primary Ab responses were induced (Fig. 3). Nasal wash IgA Abs, which were much higher than the IgG levels, will be explained by the active secretion of IgA Abs across the mucosal epithelial cells, in which dIgA binds to a polymeric Ig receptor on the basolateral surface and is carried to the apical side of the epithelial cells [13,14]. Lung wash IgG Abs, which are much higher than the IgA levels, will be explained by their transudation from serum according to the concentration gradient of IgG, which diffuse more readily across alveolar walls than across the mucosa of the upper RT [2,10]. The serum IgG Abs contained more IgG1 subclass than IgG2a (Fig. 4). Accelerated DTH responses, which established almost the same peak height as that in the case of the primary response, were induced (Fig. 5). In addition, a low CTL memory cell activity, which was detected by in vitro culture of spleen cells, was induced (Fig. 6). These results suggest that the protection against infection is mainly provided by the secondary Ab responses whose levels are higher than those of primary Ab responses and have an immediate effects of preventing infection 2 weeks after the secondary immunization. Moreover, the nasal wash IgA and the lung wash IgG titers correlated well with cross-protection against infection with variant viruses in the upper RT and protection against homologous virus infection in the lower RT, respectively (Fig. 7). These results suggest that the major protective factors among Ab and T cell-mediated immune responses, induced by the two-dose regimen using the CT112K-combined vaccine, are the IgA Abs in the upper RT and the IgG Abs in the lower RT.

Previously, we have investigated the effects of intranasal immunization with different H3N2 vaccines on cross-protection against H3N2 virus challenge in BALB/c mice immunized by the two-dose regimen, composed of administration with a primary CTB*-combined vaccine and the subsequent administration with the vaccine alone 4 weeks later, and have showed that the cross-protection was maintained for more than 12 weeks after the secondary immunization [31,52]. Thus, it is probable that the ability of the Ab responses, which were induced by the two-dose regimen using the CT112K-combined vaccine, to provide cross-protection is maintained for more than 3 months.

In the present experiments, it was shown that IgM, IgG (IgG1 and IgG2a) and IgA Ab responses mediated by Th1, Th2 and B cells [53], DTH responses mediated by Th1 cells [54,55], and CTL memory activity mediated by $CD8^+$ T cells [56,57] were induced by the two-dose regimen using the nasal CT112K-combined influenza vaccine in BALB/c mice. The Th1 memory cells induced by the two-dose regimen and involved in either the accelerated DTH responses (Fig. 5) or IgG2a Ab production (Fig. 4) are suggested to prevent influenza virus replication in mice challenged with different subtype viruses by producing IFN-γ [5,55]. CTL memory cells (Fig. 6) can also cause the accelerated elimination of infected cells in mice challenged with different subtype viruses by producing IFN-γ [54,55]. Thus, Th1 and CTL memory cells are involved in the heterosubtypic immunity, which can potentially provide cross-protection against infection by the A type viruses. However, among these Ab- and T cell-mediated immune responses induced by the two-dose regimen, the major protective factors were the IgA Abs in the upper RT and the IgG Abs in the lower RT (Figs. 3–6).

In particular, the nasal wash IgA Abs and the lung wash IgG Ab titers correlated well with cross-protection against infection with variant viruses in the upper RT and protection against homologous virus infection in the lower RT, respectively (Fig. 7). One evidence that the nasal wash IgA Abs observed in the present experiments are S-IgAs is obtained by our previous studies that anti-influenza IgA Abs, purified from the RTs of mice immunized by two-dose regimen using viral HA molecules and CTB*, were polymeric nature. In addition, the S-IgA protected nonimmune mice from influenza virus infection when administered intranasally [30,58]. Another evidence is obtained from our recent studies that polymeric Ig receptor-knockout mice, immunized intranasally with different CTB*-combined inactivated vaccines, reduced specific IgA Abs in the nasal wash [59]. Simultaneously, the immunized polymeric Ig receptor-knockout mice reduced their ability to provide protection against infection with variant viruses. The direct biological role of S-IgA in protection against virus infection has also been demonstrated in a number of studies [10,11]. Renegar and Small showed that anti-influenza HA-specific monoclonal polymeric IgA (pIgA) injected intravenously was transported more efficiently into nasal secretions than monomeric IgA (mIgA) or IgG1 [60]. They also showed that treatment of mice immunized with live influenza virus with anti-IgA Ads, but not anti-IgG and anti-IgM Abs, abrogated the protection, suggesting that IgA is a major mediator of nasal immunity [61]. In addition, Renegar et al. demonstrated that monoclonal pIgA and S-IgA are several times more effective than monoclonal monomeric IgA (mIgA) in HI and NT activities [12]. Thus, S-IgA and pIgA Abs have inherently greater antiviral activities, which are derived from their polymeric nature. These results suggest that the induction of responses of S-IgA Abs to the HA glycoprotein by the two-dose regimen, which provided cross-protection against variant viruses including those with pandemic potential, would be strategically important for improving the efficacy of currently used and parenterally administered inactivated vaccines, which provided protection against homologous virus by induction of the responses of serum IgG Abs.

The results described above are derived from experiments using the mouse, which is the most widely used animal for experimental studies of influenza virus infection. There are so many differences of anatomical structure of nose, bronchi, lungs, mucosal-associated lymphoid tissues, immunoglobulin classes, MHC, the span of life and others between humans and mice [1,15,62]. Thus, strictly speaking, immune responses obtained here using the mouse model will be different from those obtained in humans. However,

the pathology of the upper and lower RTs in the influenza mouse model, infected intranasally with mouse-adapted strains, is essentially similar to that seen in influenza in humans [1–3]. RT viral titers peak within 3–5 days and decline to undetectable levels by 10 days after infection in both mice and humans [1,5,17,43]. Infection and vaccination of humans or mice provide a high level of resistance in both upper and lower RTs, which is largely due to mucosal and systemic immune responses [2,9,10,17,18]. These facts suggest that the most suitable regimen of the nasal influenza vaccine determined in the present experiments using BALB/c mice can be applied to humans, although the suitable vaccination regimen in different strains of mice, which determines the applicability of the regimen to genetically heterogeneous humans, remains to be examined [63,64].

To evaluate the efficacy of the adjuvant-combined nasal influenza vaccine, we have previously conducted the first clinical trial by the two-dose regimen, in which currently used inactivated trivalent vaccines (140 μg) combined with LTB* (100 μg) were intranasally administered to volunteers twice, 4 weeks apart [32,33]. The results showed that the nasal LTB*-combined vaccine could induce both nasal IgA and serum IgG Ab responses to the vaccines at levels significantly higher than those induced by the nasal vaccine alone, suggesting that the nasal LTB*-combined vaccine is effective in preventing influenza. In addition, we conducted other preclinical studies, showing that 0.1 μg of CTB* or LTB* could be used as a safe nasal adjuvant without adversely affecting the brain in mice [35]. Although no serious adverse effects associated with the CTB*- or LTB*-combined vaccines were observed in the preliminary human trials, further preclinical trials on the reduction of the toxicity and allergenicity of these toxins were conducted by preparing mutant CT112K [34]. In the present study, as well as in previous studies, it was shown that the vaccine alone without the adjuvant is sufficiently effective for use as the second antigen in the two-dose regimen for providing protection and inducing the secondary Ab responses to the vaccine (Figs. 1 and 3) [28,52]. From the standpoint of safety of vaccination, using the vaccine alone as the secondary antigen in the two-dose regimen, which induces only the enhanced production of Abs to the vaccine that is required for preventing influenza, will be better than using the CT112K-combined vaccine. In addition, both 0.1 μg of CT112K and 0.1 μg of vaccine for the primary immunization and 0.1 μg of vaccine for the secondary immunization seem to be close to the minimal effective dose for providing complete protection against the virus infection. Thus, this two-dose regimen is considered to be the most suitable for the mouse model (0.1 μg/20 g body weight) which corresponds to the estimated dose per person of 100 μg/20 kg body weight. Clinical trials using CT112K will be required to confirm the effectiveness of the adjuvant-combined influenza vaccine in preventing or in attenuating illness without negative effects.

## References


[1] Murphy BR, Webster RG. Orthomyxoviruses. In: Field BN, Knipe DN, et al., editors. Virology. Philadelphia: Lippincott-Raven; 1996. p. 1397–445.

[2] Murphy BR, Clements ML. The systemic and mucosal immune response of humans to influenza A virus. Curr Top Microb Immunol 1989;146:107–16.

[3] McMichael A. Cytotoxic T lymphocytes specific for influenza virus. Curr Top Microb Immunol 1994;189:75–91.

[4] Ada GL, Jones PD. The immune response to influenza infection. Curr Top Microb Immunol 1986;128:1–54.

[5] Tamura S-I, Miyata K, Matsuo K, Asanuma H, Takahashi H, Nakajima K, et al. Acceleration of influenza virus clearance by Th1 cells in the nasal site of mice immunized intranasally with adjuvant-combined recombinant nucleoprotein. J Immunol 1996;156:3892–900.

[6] Tite JP, Hughes-Jenkins C, O'Callaghan D, Russell MS, Gao XM, Liew FY. Antiviral Immunity induced by recombinant nucleoprotein of influenza A virus. II. Protection from influenza infection and mechanism of protection. Immunology 1990;71:202–7.

[7] Waldman RH, Ganguly R. Immunity to infection on secretory surfaces. J Infect Dis 1974;130:419–40.

[8] Shvartsman YS, Zykov MP. Secretory anti-influenza immunity. Adv Immunol 1976;22:291–330.

[9] Liew FY, Russell SM, Appleyard G, Brand CM, Beale J. Cross-protection in mice infected with influenza A virus by the respiratory route is correlated with local IgA antibody rather than serum antibody or cytotoxic T cell reactivity. Eur J Immunol 1984;14:350–6.

[10] Murphy BR. Mucosal immunity to viruses. In: Ogra PL, Lamm ME, McGhee JR, Mestecky J, Strober W, Bienenstock J, editors. Handbook of mucosal immunology. San Diego, CA: Academic Press; 1994. p. 333–43.

[11] Reneger KB, Small Jr PA. Passive immunization: systemic and mucosal. In: Ogra PL, Lamm ME, McGhee JR, Mestecky J, Strober W, Bienenstock J, editors. Handbook of mucosal immunology. San Diego, CA: Academic Press; 1994. p. 347–56.

[12] Reneger KB, Jackson GD, Mestecky J. In vitro comparison of the biologic activities of monoclonal monomeric IgA, polymeric IgA, and secretory IgA. J Immunol 1998;160:1219–23.

[13] McGhee JR, Mestecky J, Dertzbaugh MT, Eldridge JH, Hirasawa M, Kiyono H. The mucosal immune system: from fundamental concepts to vaccine development. Vaccine 1992;10:75–88.

[14] Brandtzaeg P, Krajci P, Lamm ME, Kaetzl CS. Epithelial and hepatobiliary transport of polymeric immunoglobulins. In: Ogra PL, Lamm ME, McGhee JR, Mestecky J, Strober W, Bienenstock J, editors. Handbook of mucosal immunology. San Diego, CA: Academic Press; 1994. p. 113.

[15] Kuper CF, Koornastra PJ, Hameleers DMH, et al. The role of nasopharyngeal lymphoid tissue. Immunol Today 1992;13:219–24.

[16] Asanuma H, Thompson AH, Iwasaki T, Sato Y, Inaba Y, Aizawa C, et al. Isolation and characterization of mouse nasal-associated lymphoid tissue. J Immunol Methods 1997;23–131.

[17] Tamura S-I, Iwasaki T, Thompson AM, et al. Antibody-forming cells in the nasal-associated lymphoid tissue during primary influenza virus infection. J Gen Virol 1998;79:291–9.

[18] Tamura S-I, Samegai Y, Kurata H, Nagamine T, Aizawa C, Kurata T. Protection against influenza virus infection by vaccine inoculated intranasally with cholera toxin B subunit. Vaccine 1988;6:409–13.

[19] Elson CO, Ealding W. Cholera toxin feeding did not induce oral tolerance in mice and abrogated oral tolerance to an unrelated protein antigen. J Immunol 1984;133:2892–7.

[20] Lycke N, Holmgren J. Strong adjuvant properties of cholera toxin on gut mucosa immune responses to orally presented antigens. Immunology 1986;59:301–8.

[21] Clements JD, Hartzog NM, Lyon FL. Adjuvant activity of *Escherichia coli* heat-labile enterotoxin and effect on the induction of oral tolerance in mice to unrelated protein antigens. Vaccine 1988;6:269–77.

[22] Dallas WS, Kalkow S. Amino acid homology between cholera toxin and *Escherichia coli* heat-labile toxin. Nature 1980;288: 499–501.

[23] Sixma TK, Pronk SE, Kalk KW, et al. Crystal structure of a cholera toxin-related heat-labile enterotoxin from *E. coli*. Nature (Lond) 1991;351:371–7.

[24] Spanglar BD. Structure and function of cholera toxin and related *Escherichia coli* enterotoxin. Microbiol Rev 1992;56:622–47.

[25] Wilson AD, Clarke CJ, Stokes CR. Whole cholera toxin and B subunit act synergistically as an adjuvant for the mucosa immune response of mice to keyhole limpet haemocyanin. Scand J Immunol 1990;31:443–51.

[26] Tamura S-I, Yamanaka A, Shimohara M, et al. Synergistic action of cholera toxin B subunit (and *E. coli* heat-labile toxin B subunit) and a trace amount of cholera whole toxin as an adjuvant for nasal influenza vaccine. Vaccine 1994;12:419–26.

[27] Tamura S-I, Asanuma H, Tomita T, et al. *Escherichia coli* heat-labile enterotoxin B subunits supplemented with a trace amount of the holotoxin as an adjuvant for nasal influenza vaccine. Vaccine 1994;12:1083–9.

[28] Tamura S-I, Kurata H, Funato H, Nagamine T, Aizawa C, Kurata T. Protection against influenza virus infection by a two-dose regimen of nasal vaccination using vaccines combined with cholera toxin B subunit. Vaccine 1989;7:314–20.

[29] Tamura S-I, Asanuma H, Ito Y, et al. Superior cross-protective effect of nasal vaccination to subcutaneous inoculation with influenza HA vaccine. Eur J Immunol 1992;22:477–81.

[30] Tamura S-I, Funato H, Hirabayashi Y, et al. Cross-protection against influenza A virus infection by passively transferred respiratory tract IgA antibodies to different haemagglutinin molecules. Eur J Immunol 1991;21:1337–44.

[31] Tamura S-I, Ito Y, Asanuma H, et al. Cross-protection against influenza virus infection afforded by trivalent inactivated vaccines inoculated intranasally with cholera toxin B subunit. J Immunol 1992;149:981–8.

[32] Hashigucci K, Ogawa H, Ishidate T, et al. Antibody responses in volunteers induced by nasal influenza vaccine combined with *Escherichia coli* heat-labile enterotoxin B subunit containing a trace amount of the holotoxin. Vaccine 1996;14:113–9.

[33] Hashigucci K, Tamura S-I, Kurata T, Kamiya H, Ishidate T. Efficacy of nasal influenza vaccine combined with *Escherichia coli* heat-labile enterotoxin B subunit containing a trace amount of the holotoxin in healthy volunteers. J Jpn Assoc Infect Dis 1997;71:153–61.

[34] Hagiwara Y, Iwasaki T, Asanuma H, et al. Effects of intranasal administration of cholera toxin (or *Escherichia coli* heat-labile enterotoxin) subunits supplemented with a trace amount of the holotoxin on the brain. Vaccine 2001;19:1652–60.

[35] van Ginkel FW, Jackson RJ, Yuki Y, McGhee JR. Cutting edge: the mucosal adjuvant cholera toxin redirects vaccine proteins into olfactory tissues. J Immunol 2000;165:4778–82.

[36] Komase K, Tamura S-I, Matsuo K, et al. Mutants of *Escherichia coli* heat-labile enterotoxin as an adjuvant for nasal influenza vaccine. Vaccine 1998;16:248–54.

[37] Yamamoto S, Takeda Y, Yamamoto M, et al. Mutants in the ADP-ribosyltransferase cleft of cholera toxin lack diarrheagenicity but retain adjuvanticity. J Exp Med 1997;185:1203–10.

[38] Yamamoto S, Kiyono H, Yamamoto M, et al. A nontoxic mutant of cholera toxin elicits Th2-type responses for enhanced mucosal immunity. Proc Natl Acad Sci USA 1977;94:5267–72.

[39] Hagiwara Y, Komase K, Chen Z, et al. Mutants of cholera toxin as an effective and safe adjuvant for nasal influenza vaccine. Vaccine 1999;17:2918–26.

[40] Uesaka Y, Osuka T, Lin Z, et al. Simple method of purification of *Escherichia coli* heat-labile enterotoxin and cholera toxin using immobilized galactose. Microb Pathogen 1994;16:71–6.

[41] Nakamura S, Morita T, Iwanaga S, Niwa M, Takashi K. A sensitive substrate for the clotting enzyme in horseshoe crab hemocytes. J Biochem 1977;81:1567–9.

[42] Davenport FM, Hennessy AV, Brandon FM, Webster RG, Barrett CD, Lease GO. Comparison of serologic and febrile responses in humans to vaccination with influenza A viruses or their hemagglutinin. J Lab Clin Med 1964;63:5.

[43] Yetter RA, Lehrer S, Ramphal R, Small Jr PA. Outcome of influenza infection: effect of site of initial infection and heterotypic immunity. Infect Immun 1980;29:654.

[44] Tobita K, Sugiura A, Enomote C, Furuyama M. Plaque assay and primary isolation of influenza A viruses in an established line of canine kidney cells (MDCK) in the presence of trypsin. Med Microbiol Immunol (Berl) 1975;162:9.

[45] Tobita K. Permanent canine kidney (MDCK) cells for isolation and plaque assay of influenza B viruses. Med Microbiol Immunol (Berl) 1975;162:23.

[46] Czerkinsky C, Nilsson LA, Nygren H, Ouchterlony O, Tarkowski A. A solid-phase enzyme-linked immunospot (ELISPOT) assay for enumeration of specific antibody-secreting cells. J Immunol Methods 1983;65:5–13.

[47] Lycke N. A sensitive method for the detection of specific antibody production in different isotypes from single lamina propria plasma cells. Scand J Immunol 1986;24:393–403.

[48] Phelan MA, Mayner RE, Bucker DJ, Ennis FA. Purification of influenza virus glycoproteins for the preparation and standardization of immunological potency testing reagents. J Biol Standard 1980;8:233–42.

[49] Bennink JR, Yewdell JW, Smith GL, Moss B. Recognition of cloned influenza virus hemagglutinin gene products by cytotoxic T lymphocytes. J Virol 1986;57:786–91.

[50] Bender BS, Ulmer JB, DeWitt CM, et al. Immunogenicity and efficacy of DNA vaccines encoding influenza A proteins in aged mice. Vaccine 1998;16:1746–55.

[51] Kadowaki S-E, Chen Z, Asanuma H, Aizawa C, Kurata T, Tamura S-I. Protection against influenza virus infection in mice immunized by administration of hemagglutinin-expressing DNAs with electroporation. Vaccine 2000;18:2779–88.

[52] Tamura S-I, Kurata T. Intranasal immunization with influenza vaccine. In: Kiyono H, Ogra PL, McGhee JR, editors. Mucosal vaccines. San Diego, CA: Academic Press; 1996. p. 425–36 [Chapter 32].

[53] Mosmann TR, Coffman RL. Heterogeneity of cytokine secretion patterns and functions of helper T cells. Adv Immunol 1989;46: 111–47.

[54] McDermott MR, Lukacher AE, Braciale VL, Braciale TJ, Bienenstock J. Characterization and in vivo distribution of influenza-virus-specific T lymphocytes in the murine respiratory tract. Am Rev Resp Dis 1987;135:245–9.

[55] Taylor PM, Esquivel F, Askonas BA. Murine $CD4^+$ T cell clones vary in function in vitro and in influenza virus infection in vivo. Int Immunol 1990;2:323–8.

[56] Flynn KJ, Belz GT, Altman JD, Ahmed R, Woodland DL, Doherty PC. Virus-specific $CD8^+$ T cells in primary and secondary influenza pneumonia. Immunity 1998;8:683–91.

[57] Flynn KJ, Riberdy JM, Christensen JP, Altman JD, Doherty PC. In vivo proliferation of naive and memory influenza-specific $CD8^+$ T cells. Proc Natl Acad Sci USA 1999;96:8597–602.

[58] Tamura S-I, Funato H, Hirabayashi Y, et al. Functional role of respiratory tract haemagglutinin-specific IgA antibodies in protection against influenza. Vaccine 1990;8:479–86.

[59] Asahi Y, Yoshikawa T, Watanabe I. Protection against influenza virus infection in polymeric Ig receptor-knockout mice immunized intranasally with adjuvant-combined vaccine. J Immunol 2002;168: 2930–8.

[60] Renegar KB, Small Jr PA. Passive transfer of local immunity to influenza virus infection by IgA antibody. J Immunol 1991;146: 1972–8.
[61] Renegar KB, Small Jr PA. Immunoglobulin A mediation of murine nasal anti-influenza virus immunity. J Virol 1991;65:2146–8.
[62] Perry M, Whyte A. Immunology of the tonsils. Immunol Today 1998;19:410–21.
[63] Tamura S-I, Kurata T. A proposal for safety standards for human use of cholera toxin (or *Escherichia coli* heat-labile enterotoxin) derivatives as an adjuvant of nasal inactivated influenza vaccine. Jpn J Infect Dis 2000;53:98–106.
[64] Chen Z, Kurata T, Tamura S-I. Identification of effective constituents of influenza vaccine by immunization with phasmid DNAs encoding viral proteins. Jpn J Infect Dis 2000;53:219–28.

ACADEMIC PRESS

Biochemical and Biophysical Research Communications 297 (2002) 329–334

BBRC

www.academicpress.com

# IL-15 up-regulates iNOS expression and NO production by gingival epithelial cells☆

Manabu Yanagita,[a] Yoshio Shimabukuro,[a] Takenori Nozaki,[a] Naoko Yoshimura,[a] Junko Watanabe,[a] Hiroko Koide,[a] Mami Terakura,[a] Teruyuki Saho,[a] Masahide Takedachi,[a] Myoung-Ho Jang,[b] Hiroshi Kiyono,[b] and Shinya Murakami[a,*]

[a] *Department of Periodontology, Division of Oral Biology and Disease Control, Osaka University Graduate School of Dentistry, 1-8 Yamadaoka, Suita, Osaka 565-0871, Japan*

[b] *Department of Mucosal Immunology, Research Institute for Microbial Diseases, Osaka University, 1-8 Yamadaoka, Suita, Osaka 565-0871, Japan*

Received 22 August 2002

**Abstract**

To investigate the biological activity of epithelial cells in view of host defense, we analyzed the mRNA expression of inducible NOS (iNOS) as well as NO production by human gingival epithelial cells (HGEC) stimulated with IL-15. RT-PCR analysis revealed that HGEC expressed IL-15 receptor α-chain mRNA. In addition, stimulation with IL-15 enhanced iNOS expression by HGEC through an increase of both mRNA and protein levels. Moreover, IL-15 up-regulated the production of $NO_2^-/NO_3^-$, a NO-derived stable end product, from HGEC. The enhanced NO production by IL-15 was inhibited by AMT, an iNOS-specific inhibitor. These results suggest that IL-15 is a potent regulator of iNOS expression by HGEC and involved in innate immunity in the mucosal epithelium. © 2002 Elsevier Science (USA). All rights reserved.

*Keywords:* iNOS; NO; Gingival epithelial cells; Interleukin 15; Periodontal diseases

Epithelial cells lining the mucosal lumen are continuously exposed to environment antigen including commensal microflora, pathogens, and allergens. Thus, they populate potential initial sites of infection and inflammation. Recent studies have shown that epithelial cells provide not only a physiological barrier against bacteria, viruses, and food antigens, but also function as immunocompetent cells that participate in the induction and regulation of immune response and inflammation. In fact, epithelial cells are known to produce pro-inflammatory chemoattractant cytokines (e.g., IL-8, TNF-α, IFN-γ, IL-1β, and MCP-1) and immunoregulatory cytokines (e.g., IL-7, SCF, and IL-15) [1,2].

Among those cytokines, IL-15, which was originally identified as a T cell growth factor derived from a CV-1/EBNA kidney epithelial cell line, shows multiple biological activities, such as activation of NK cells, macrophages (Mϕ), and T cells (especially, intraepithelial γδT cells), and isotype-class-switching of tonsillar B cells [3–5]. Previous studies have shown that IL-15 stimulates the proliferation of intestinal epithelial cells [6]. In addition, we recently reported that IL-15 selectively regulates the differentiation of B-1 cells for IgA responses [6]. Although IL-15 shares many biological roles with IL-2, IL-15 expression has been shown to be produced by various cell types, such as intestinal epithelial cells, Mϕ, fibroblasts, and skeletal muscle cells [3–5,7], in contrast to the relatively limited expression of IL-2 by T cells. In addition, IL-15 receptors (IL-15R) are known to be expressed in a variety of tissues, including epithelial cells [8], B-1 cells, and NK cells [4].

Nitric oxide (NO), shown to have physiological and pathophysiologic roles in neurotransmission, blood pressure homeostasis, and immunological responses, is produced from L-arginine by NO synthase (NOS) [9].

☆ *Abbreviations:* cDNA, complimentary DNA; HGEC, human gingival epithelial cells; IEL, intestinal intraepithelial lymphocyte; NOS, nitric oxide synthase.

* Corresponding author. Fax: +81-6-6879-2934.
*E-mail address:* ipshinya@dent.osaka-u.ac.jp (S. Murakami).

0006-291X/02/$ - see front matter © 2002 Elsevier Science (USA). All rights reserved.
PII: S0006-291X(02)02201-5

Thus far, three isoforms of NOS have been cloned, two (endothelial NOS, eNOS; neural NOS, nNOS) of which are expressed in a constitutive manner in neural and endothelial cells [10]. On the other hand, the expression of inducible NOS (iNOS), seen in such diverse cell types as Mϕ, hepatocytes, and keratinocytes, is induced by LPS or cytokine stimulation and has an ability to generate large amounts of NO [11–17].

It has been reported that cytokine- or LPS-induced iNOS is involved in the abrogation of intracellular pathogen and inflammatory responses [17–19]. Furthermore, it was demonstrated that NO produced by intestinal epithelial cells is involved in host defense against lumen pathogens [14]. Interestingly, iNOS expression was also observed in the gingival epithelial basal layers of non-inflamed and inflamed periodontal tissues [15]. However, the molecular mechanism(s) for the regulation of iNOS and NO expression by human gingival epithelial cells (HGEC) is/are not fully clarified. In the present study, we examined the effect of IL-15 on iNOS and NO production by HGEC, and, consequently, demonstrated for the first time that IL-15 is a potent inducer of mRNA expression in iNOS and NO production in HGEC, which may function to confront numerous bacteria in dental plaque.

## Materials and methods

*Cells and reagents.* All human subjects participated in this study after providing informed consent with the experimental protocol that was reviewed and approved by the Institutional Review Board of the Osaka University Faculty of Dentistry. Gingival specimens obtained during periodontal surgery were minced and treated with 0.4% Dispase II (Boehringer–Mannheim, GmbH, Germany) overnight at 4 °C. The epidermal sheet was separated and trypsinized with 0.05% trypsin–EDTA (Bioconcept, Allschwill, Switzerland) to disperse single cells, after which they were seeded and allowed to form subcultures. Human gingival epithelial cells (HGEC) were grown in Humedia-KG2 (KURABO, Osaka, Japan) with a final concentration of 0.5 μg/ml hydrocortisone, 10 μg/ml insulin, 0.4% v/v bovine pituitary extract, 0.1 ng/ml hEGF, 50 μg/ml gentamicin, and 50 ng/ml amphotericin B. HGEC were then passed by trypsinization and used for experiments at passages 1–3. In addition, several lines of cultured primary HGEC were transformed with SV-40 T-antigen [13], after which one clone, epi 4, was finally established. Clone epi 4 was also maintained in HuMedia-KG2 with supplements. Recombinant human IL-15 (Peprotech, Rocky Hill, NJ), recombinant IL-1β, IL-8, TNF-α, IFN-γ (Genzyme, Cambridge, MA), LPS purified from *Escherichia coli* (Sigma, St. Louis, MO), and AMT hydrochloride (2-amino-5,6-dihydro-6-methyl-4*H*-1,3-thiazine hydrochloride) (Research Biochemicals International, Natick, MA) were obtained commercially and used according to the instruction.

*RT-PCR for iNOS- and IL-15 receptor α-chain-specific mRNA.* Oligonucleotide PCR primers specific for iNOS, IL-15 receptor α-chain, and glyceraldehyde-3-phosphate dehydrogenase (GAPDH) were synthesized at Takara Shuzo (Shiga, Japan). The primers for iNOS were: 5′-ATG GAA CAT CCC AAA TAC GA-3′ and (antisense) 5′-GTC GTA GAG GAC CAC TTT GT-3′, those for IL-15 receptor α-chain: 5′-GTC AAG AGC TAC AGC TTG TAC-3′ and (antisense) 5′-GGT GAG CTT TCT CCT GGA G-3′ [20], while those for GAPDH were: 5′-TGA AGG TCG GAG TCA ACG GAT TTG GT-3′ and (antisense) 5′-CAT GTG GGC CAT GAG GTC CAC CAC-3′ [20,21]. HGEC were cultured with an optimal concentration of the indicated cytokines for 24 h, then harvested after stimulation, and thoroughly washed with PBS. Total RNA was prepared by homogenization in RNAzol (Cinna/Biotex, Friendswood, TX). Recovered RNA was resuspended in 0.1% DEPC-treated water. cDNA synthesis was performed with 1 μg RNA in a 40 μl cDNA synthesis reaction mixture containing 5.2 μl DEPC-treated water, 4 μl of 10× PCR buffer II (100 mM Tris–HCl, pH 8.3, 500 mM KCl; Perkin–Elmer Cetus, Norwalk, CT), 6 μl of 25 mM $MgCl_2$, 4 μl of 10 mM dNTP (Takara Shuzo), 0.4 μl of 20 U/ml RNase inhibitor (Takara Shuzo), and 1 μl of 50 U/ml M-MLV reverse transcriptase (Takara Shuzo). The mixture was incubated at 37 °C for 60 min, after which all samples were heated to 99 °C for 5 min for inactivation of the reverse transcriptase. Products were diluted to a final volume of 130 μl.

PCR were performed in a final volume of 50 μl containing 4 μl of 10× PCR buffer, 2.5 μl of 25 mM $MgCl_2$, 32.25 μl of sterile water, 0.25 μl of 5 U/μl Ampli Taq DNA polymerase (Perkin–Elmer Cetus), and 0.5 μl of 20 μM of each primer. All reactions were subjected to different cycles of amplification by means of a programmed thermal cycler (Perkin–Elmer Cetus) under the following conditions: 94 °C for 45 s, 59 °C for 45 s, and 72 °C for 2 min. The 7 μl samples were analyzed on 1.8% agarose–ethidium bromide gels run at 100 V for 30 min.

*Nitrate and nitrite estimation.* The accumulated levels of nitrate and nitrite resulting from NO produced by IL-15-stimulated HGEC were measured, as NO is rapidly converted into these two stable end products [22]. HGEC were incubated at a density of $10^5$/well in 3 ml of HuMedia-KG2 with IL-15 (100 ng/ml) in the presence or absence of AMT hydrochloride ($1 \times 10^{-4}$ M) at 37 °C for 48 h. The culture supernatants were collected and centrifuged at 10,000 rpm for 10 min at 4 °C, after which the supernatants were harvested and subjected to analyses of NO (nitrate and nitrite) production using Nitrate/Nitrite Fluorometric Assay Kits (Cayman Chemical, Ann Arbor, MI) according to manufacturer's instructions.

*Intracellular iNOS expression.* Intracellular iNOS protein was detected by FACS [22]. HGEC were incubated at a density of $10^5$/well in 3 ml HuMedia-KG2 with IL-15 (100 ng/ml) at 37 °C for 48 h. To assess the influence of IL-15/IL-15R interaction, HGEC were incubated in the presence or absence of cytochalasin D (10 ng/ml). For detection of iNOS, cells were harvested, fixed using Cytofix solution (Pharmingen, San Diego, CA), and incubated at 4 °C for 15 min. After washing with Perm/wash (Pharmingen), the cells were incubated with 1:1000 diluted primary anti-iNOS monoclonal antibody (Transduction Laboratory, Lexington, KY) at 4 °C for 30 min. The cells were then washed and incubated with 1:1000 diluted Alexa488-labelled goat anti-mouse IgG antibodies (Molecular Probes, Eugene, OR) at 4 °C for 30 min. Immunofluorescent cell staining was analyzed using flow cytometry (FACS calibur, Becton–Dickinson, Franklin Lakes, NJ). All staining included negative controls from which the primary Abs were omitted.

## Results

### *Detection of IL-15 receptor α-chain in HGEC by RT-PCR*

IL-15 receptor is composed of a distinct α-chain and the same β- and γ-chain with IL-2 receptor. Therefore, we first examined the expression of IL-15 receptor α-chain mRNA in HGEC and epi 4. As shown in Fig. 1, IL-15 receptor α-chain mRNA expression was observed in cultured HGEC and epi 4.

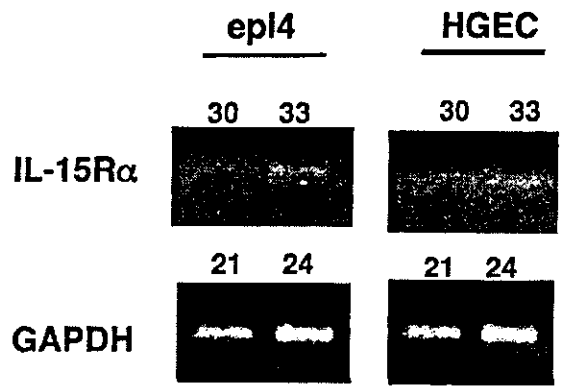


Fig. 1. Detection of IL-15 receptor α-chain mRNA in cultured HGEC by RT-PCR. Total RNA was prepared from cultured HGEC and epi 4. cDNA syntheses by RT and PCR were performed. Representative results of one of the three independent experiments are shown. The number of PCR cycles is shown above each lane.

*Induction of iNOS mRNA expression following IL-15 stimulation*

Without stimulation, iNOS mRNA was not detected by RT-PCR in HGEC (Fig. 2). However, stimulation with IL-15 induced the expression of iNOS mRNA in a dose-dependent manner. The levels of IL-15-induced iNOS were similar to those exposed to a combination of IFN-γ and IL-8, or IL-1β and TNF-α, which are known to induce iNOS mRNA expression in intestinal epithelial cells, bronchial epithelial cells, and Mϕ [11,12,14,16,17] (Fig. 2).

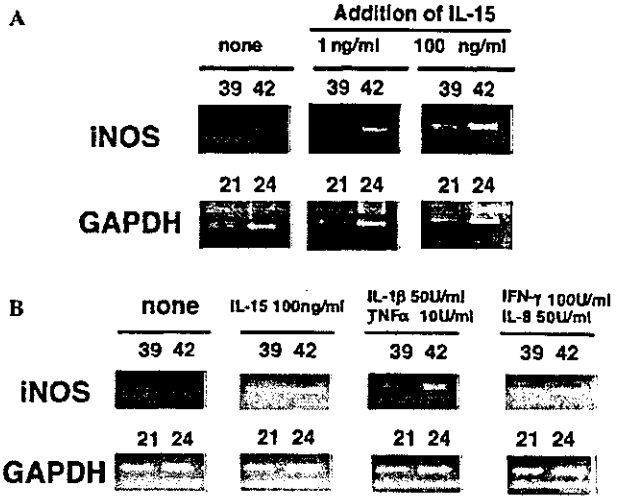


Fig. 2. Detection of IL-15-induced iNOS mRNA in cultured HGEC by RT-PCR. HGEC were incubated for 24 h in the presence or absence of (A) 1 or 100 ng/ml IL-15; (B) 100 ng/ml IL-15, 50 U/ml IL-1β plus 10 U/ml TNF-α, 100 U/ml IFN-γ plus 50 U/ml IL-8. Representative results of one of the three independent experiments are shown. The number of PCR cycles is shown above each lane.

*Detection of iNOS protein in HGEC by FACS*

To examine the iNOS expression in HGEC at the protein level, we performed intracellular protein staining and analyzed the result using flow cytometry. As shown in Fig. 3, non-stimulated HGEC expressed a low level of iNOS protein. However, when stimulated with IL-15, the expression of iNOS protein was clearly up-regulated. Interestingly, the IL-15-induced iNOS expression was down-regulated when the IL-15-stimulated HGEC were simultaneously treated with cytochalasin D, a disrupter of the cytoskeleton actin element.

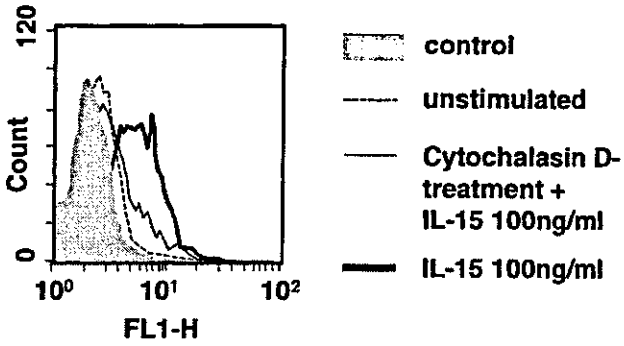


Fig. 3. Cytofluorometry analysis of iNOS protein expression in IL-15-treated HGEC. HGEC were incubated for 48 h with or without 100 ng/ml IL-15 in the presence or absence of cytochalasin D (10 ng/ml). The cells were then stained for expression of iNOS protein as described in Materials and methods. Dotted, thin, and thick lines represent flow cytometric profile of iNOS expression in the non-stimulated HGEC, cytochalasin D plus IL-15 stimulated, and IL-15 stimulated HGEC, respectively. Representative results of one of the three independent experiments are shown.

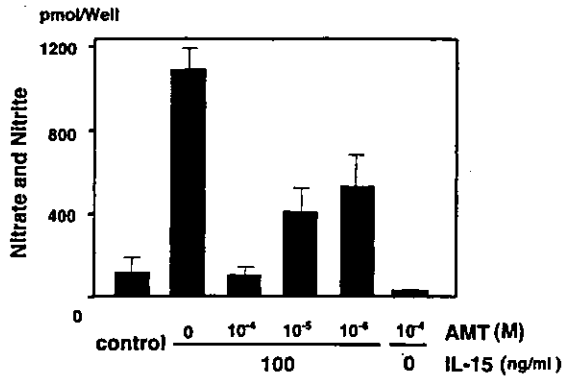


Fig. 4. The effect of IL-15 on NO production in HGEC. HGEC were incubated for 48 h with or without 100 ng/ml IL-15 in the presence or absence of AMT ($1 \times 10^{-4}$ M). Nitrate and nitrite levels in the culture supernatants were determined as described in Materials and methods. Representative results of one of the three independent experiments are shown.

*NO production by HGEC*

We next examined whether IL-15 could induce NO production by HGEC. Monolayers of HGEC were cultured with IL-15 for 48 h and nitrate and nitrite production in the culture supernatants was examined. As shown in Fig. 4, non-stimulated HGEC demonstrated marginal NO production (value 74.5 pM/well), whereas IL-15 clearly increased NO production. The IL-15-induced NO production by HGEC was inhibited by AMT, a selective inhibitor of iNOS [23], in a dose-dependent manner up to 15 M, which completely suppressed NO production.

## Discussion

Previous studies have found that keratinocytes can be induced to express iNOS by stimulation with IL-1β, IL-8, TNF-α, IFN-γ, or LPS as well as their combinations [11,14,24]. Although an immunohistochemical study demonstrated iNOS expression by gingival fibroblasts and basal keratinocytes [15], the mechanism by which iNOS expression is induced in HGEC remains to be clarified. Prior to the present study, we found that IL-15 protein was expressed in a constitutive manner in basal epithelial keratinocytes in healthy human gingivae, and that IL-15 and IL-15Rα-chain mRNA could be detected in HGEC by RT-PCR analysis (unpublished data and Fig. 1), which led us to explore the effects of IL-15 on iNOS expression in HGEC.

Umemura et al. [25] reported higher level of iNOS mRNA expression in the peritoneal macrophages in IL-15 transgenic mice after stimulation of *Mycobacterium bovis* bacillus Calmette–Guérin (BCG), compared with those of wild mice. Another study showed both iNOS and IL-15 mRNA expressions were up-regulated in mouse dendritic cells after stimulation of LPS or *Propionebacterium acnes* [26]. These studies suggested that IL-15 may be involved in iNOS expression on other cell types. In this study, we directly demonstrated for the first time that IL-15 has the ability to induce iNOS expression and NO production by using HGEC.

Because of the confrontation with a plethora of pathogens and antigens as the first line of host defense, epithelial cells lining the mucosal lumen secrete numerous cytokines and bioactive molecules. To this end, it was shown that bacterial invasion induced IL-7R expression in a colonic epithelial cell line, T84, and suggested that IL-7 and IL-7R might be involved in the modulation of mucosal inflammation after bacterial invasion [27]. A similar mechanism may occur in the case of IL-15/IL-15R interactions, since IL-15 is known to be produced by epithelial cells [6,28]. The co-stimulatory interaction between CD40 ligand (CD154) expressed on activated T cells and its CD40 receptor on epithelial cells leads to the up-regulation of IL-15 production by tubular epithelial cells [29]. Since numerous monocytes/macrophages and activated T cells were also detected in inflamed periodontal lesions [30], it is likely that, in addition to the chemotactic activity of IL-15 for T lymphocytes, gingival epithelial cells are influenced by IL-15 in an autocrine and paracrine manner and can be provoked to acquire a variety of biological activities. It was shown that invasion of *Listeria* resulted in the up-regulation of IL-15 expression by epithelial cells. Thus, it is interesting to determine if IL-15R expression occurs in gingival epithelial cells after bacterial challenge and further investigation is proceeding to clarify IL-15 and IL-15R interaction in oral cavity for the development of inflammation, as well as the signaling mechanism of iNOS expression after IL-15 stimulation.

In healthy condition, NO induced by IL-15 or other factors may function bactericidally. However, continuous and/or excessive production of NO may provoke the promotion of inflammation and tissue destruction [16,29]. In fact, it has been reported that epithelial cells highly express iNOS at both mRNA and protein levels in inflammatory lesions, including those of periodontitis [15]. Although the physiological and pathophysiologic roles of iNOS expression in periodontal lesions are not yet fully defined, it is expected that hyperproduction of NO in inflamed periodontal lesions may be involved in epithelial barrier dysfunction and alveolar bone resorption.

It was shown that inflammatory cytokines such as IFNγ, IL-1, IL-8, and TNFα were able to induce iNOS and NO production by epithelial cells [17,31–33]. Our present findings provided new evidence that IL-15 is also a potent regulatory cytokine for the stimulation of iNOS and NO cascade. Based on the titer to induce iNOS and NO expression (Fig. 2), it is expected that the effect of IL-15 is no less than those of the above-mentioned cytokines. Interestingly, we recently showed that treatment of HGEC with adenosine, an endogenous nucleoside with an abundance of biological actions, resulted in the elevation of iNOS mRNA and NO production [21]. Thus, it may be speculated that several regulatory mechanisms of iNOS expression by HGEC exist, which may function protectively or destructively in periodontal tissues.

IL-15 acts via IL-15R, which shares β- and γ-subunit with IL-2R. However, unlike IL-2R, IL-15R expression is widely distributed throughout a variety of tissues and cells. It remains uncertain what kind of intracellular signal transduction is involved in IL-15R-mediated iNOS expression in HGEC, though several signaling pathways have been implicated in the up-regulation of iNOS mRNA. Among these factors, NF-κB is a pivotal transcription inducer of iNOS expression in various cells. A recent study revealed that the cytoplasmic domain of IL-15R possesses the TNFR-associated factor-2

(TRAF2, a transducer of TNF-α-mediated NF-κB activation) binding motif and that ligation of IL-15 with IL-15R resulted in NF-κB activation via p-IκB phosphorylation [34]. These results suggest that NF-κB may be associated with the IL-15-induced iNOS elevation in HGEC.

Treatment of epi 4 with cytochalasin D, a disrupter of the cytoskeleton actin element, resulted in prevention of iNOS expression (Fig. 3), and depolymerization of the actin cytoskeleton has been reported to inhibit ERK1/2 activation [35] and PKA action [36]. Thus, it is likely that these signal pathways, which involve polymerization of the actin filament, may also mediate iNOS expression through the interaction of IL-15 and IL-15R, though the precise mechanisms by which IL-15R mediates iNOS expression still remain to be explained.

It is possible that endothelial cells and the fibroblasts underlying gingival epithelial cells are also influenced by IL-15 generated from gingival epithelial cells. A recent report has revealed that stimulation with IL-15 increased hyaluronan synthesis by endothelial cells [37] and gingival fibroblasts (data not shown). Since hyaluronan is known to function as a scavenger of NO derivatives such as peroxynitrite [38], which exerts deleterious effects on host cells, the IL-15-induced hyaluronan generation by endothelial cells and fibroblasts may contribute to the prevention of NO-associated tissue damage.

In summary, our findings suggest that IL-15 is a potent regulator of iNOS expression in epithelial keratinocytes. Further study is needed to clarify the in vivo roles of NO derived from gingival epithelial cells.

## Acknowledgments

We thank the members of the Department of Periodontology, Osaka University Graduate School of Dentistry for their constructive discussion. This work was supported in part by Grants-in-Aid from the Japan Society for the Promotion of Science and the Ministry of Health and Welfare (Nos. 11470461, 12672034, and 13307061). M.Y. is a recipient of the Fellowship Grant of the Japan Society for the Promotion of Science.

## References

[1] M.F. Kagnoff, L. Eckmann, Epithelial cells as sensors for microbial infection, J. Clin. Invest. 100 (1997) 6–10.
[2] D.W. McGee, in: Mucosal Immunology, Academic Press, San Diego, CA, 1999, pp. 559–573.
[3] A. Ma, D.L. Boone, J.P. Lodolce, The pleiotropic functions of interleukin 15: not so interleukin 2-like after all, J. Exp. Med. 191 (2000) 753–756.
[4] Y. Tagaya, R.N. Bamford, A.P. DeFilippis, T.A. Waldmann, IL-15: a pleiotropic cytokine with diverse receptor/signaling pathways whose expression is controlled at multiple levels, Immunity 4 (1996) 329–336.
[5] T.A. Waldmann, Y. Tagaya, The multifaceted regulation of interleukin-15 expression and the role of this cytokine in NK cell differentiation and host response to intracellular pathogens, Annu. Rev. Immunol. 49 (1999) 1719–1749.
[6] H.C. Reinecker, R.P. MacDermott, S. Mirau, A. Dignass, D.K. Podolsky, Intestinal epithelial cells both express and respond to interleukin 15, Gastroenterology 111 (1996) 1706–1713.
[7] T. Hiroi, M. Yanagita, N. Ohta, G. Sakaue, H. Kiyono, IL-15 and IL-15 receptor selectively regulate differentiation of common mucosal immune system-independent B-1 cells for IgA responses, J. Immunol. 165 (2000) 4329–4337.
[8] J.G. Giri, S. Kumaki, M. Ahdieh, D.J. Friend, A. Loomis, K. Shanebeck, R. DuBose, D. Cosman, L.S. Park, D.M. Anderson, Identification and cloning of a novel IL-15 binding protein that is structurally related to the α chain of the IL-2 receptor, EMBO J. 14 (1995) 3654–3663.
[9] S. Moncada, A. Higgs, The L-arginine–nitric oxide pathway, N. Engl. J. Med. 329 (1993) 2002–2012.
[10] C.R. Lyons, The role of nitric oxide in inflammation, Adv. Immunol. 60 (1995) 323–371.
[11] K. Asano, C.B. Chee, B. Gaston, C.M. Lilly, C. Gerard, J.M. Drazen, J.S. Stamler, Constitutive and inducible nitric oxide synthase gene expression, regulation, and activity in human lung epithelial cells, Proc. Natl. Acad. Sci. USA 91 (1994) 10089–10093.
[12] L. Eckmann, F. Laurent, T.D. Langford, M.L. Hetsko, J.R. Smith, M.F. Kagnoff, F.D. Gillin, Nitric oxide production by human intestinal epithelial cells and competition for arginine as potential determinants of host defense against the lumen-dwelling pathogen *Giardia lamblia*, J. Immunol. 164 (2000) 1478–1487.
[13] M. Fried, C. Prives, in: M. Botchan, T. Grodzicker, P. Sharp (Eds.), Cancer Cells 4: DNA Tumor Viruses, Cold Spring Harbor Laboratory, Cold Spring Harbor, New York, 1986, pp. 1–16.
[14] G. Hoffmann, J. Grote, F. Friedrich, N. Mutz, W. Schobersberger, The pulmonary epithelial cell line L 2 as a new model for an inducible nitric oxide synthase expressing distal airway epithelial cell, Biochem. Biophys. Res. Commun. 217 (1995) 575–583.
[15] H.K. Kendall, H.R. Haase, Y. Xiao, M.P. Barthold, Nitic oxide synthase type-II is synthesized by human gingival tissue and cultured human gingival fibroblasts, J. Periodont. Res. 35 (2000) 194–200.
[16] C. Nathan, Inducible nitric oxide synthase: what difference does it make? J. Clin. Invest. 100 (1997) 2417–2423.
[17] A.L. Salzman, T. Eaves Pyles, S.C. Linn, A.G. Denenberg, C. Szabo, Bacterial induction of inducible nitric oxide synthase in cultured human intestinal epithelial cells, Gastroenterology 114 (1998) 93–102.
[18] T. Eaves Pyles, K. Murthy, L. Liaudet, L. Virag, G. Ross, F.G. Soriano, C. Szabo, A.L. Salzman, Flagellin, a novel mediator of Salmonella-induced epithelial activation and systemic inflammation: IκB α degradation, induction of nitric oxide synthase, induction of proinflammatory mediators, and cardiovascular dysfunction, J. Immunol. 166 (2001) 1248–1260.
[19] I.P. Oswald, I. Eltoum, T.A. Wynn, B. Schwartz, P. Caspar, D. Paulin, A. Sher, S.L. James, Endothelial cells are activated by cytokine treatment to kill an intravascular parasite, *Schistosoma mansoni*, through the production of nitric oxide, Proc. Natl. Acad. Sci. USA 91 (1994) 999–1003.
[20] N. Kumaki, D.M. Anderson, D. Cosman, S. Kumaki, Expression of interleukin-15 and its receptor by human fetal retinal pigment epithelial cells, Curr. Eye Res. 15 (1996) 876–882.
[21] S. Murakami, N. Yoshimura, H. Koide, J. Watanabe, M. Takedachi, M. Terakura, M. Yanagita, T. Hashikawa, T. Saho, Y. Shimabukuro, H. Okada, Activation of adenosine receptor enhanced iNOS mRNA expression by gingival epithelial cells, J. Dent. Res. 81 (2002) 236–240.

[22] S. Moncada, R.M. Palmer, E.A. Higgs, Nitric oxide: physiology, pathophysiology, and pharmacology, Pharmacol. Rev. 43 (1991) 109–142.
[23] M. Nakane, V. Klinghofer, J.E. Kuk, J.L. Donnelly, G.P. Budzik, J.S. Pollock, F. Basha, G.W. Carter, Novel potent and selective inhibitors of inducible nitric oxide synthase, Mol. Pharmacol. 47 (1995) 831–834.
[24] D. Bruch Gerharz, K. Fehsel, C. Suschek, G. Michel, T. Ruzicka, V. Kolb Bachofen, A proinflammatory activity of interleukin 8 in human skin: expression of the inducible nitric oxide synthase in psoriatic lesions and cultured keratinocytes, J. Exp. Med. 184 (1996) 2007–2012.
[25] M. Umemura, H. Nishimura, K. Hirose, T. Matsuguchi, Y. Yoshikai, Overexpression of IL-15 in vivo enhances protection against *Mycobacterium bovis* bacillus Calmette–Guérin infection via augmentation of NK and T cytotoxic 1 responses, J. Immunol. 167 (2001) 946–956.
[26] A.S. MacDonald, A.D. Straw, B. Bauman, E.J. Pearce, CD8-dendritic cell activation status plays an integral role in influencing Th2 response development, J. Immunol. 167 (2001) 1982–1988.
[27] K. Yamada, M. Shimaoka, K. Nagayama, T. Hiroi, H. Kiyono, T. Honda, Bacterial invasion induces interleukin-7 receptor expression in colonic epithelial cell line, T84, Eur. J. Immunol. 27 (1997) 3456–3460.
[28] M. Weiler, B. Rogashev, T. Einbinder, M.J. Hausmann, J. Kaneti, C. Chaimovitz, A. Douvdevani, Interleukin-15, a leukocyte activator and growth factor, is produced by cortical tubular epithelial cells, J. Am. Soc. Nephrol. 9 (1998) 1194–1201.
[29] M. Weiler, L. Kachko, C. Chaimovitz, C. Van Kooten, A. Douvdevani, CD40 ligation enhances IL-15 production by tubular epithelial cells, J. Am. Soc. Nephrol. 12 (2001) 80–87.
[30] H. Okada, Y. Shimabukuro, Y. Kassai, H. Ito, T. Matsuo, S. Ebisu, Y. Harada, The function of gingival lymphocytes on the establishment of human periodontitis, Adv. Dent. Res. 2 (1988) 364–367.
[31] I. Arany, M.M. Brysk, H. Brysk, S.K. Tyring, Regulation of inducible nitric oxide synthase mRNA levels by differentiation and cytokines in human keratinocytes, Biochem. Biophys. Res. Commun. 220 (1996) 618–622.
[32] J.U. Igietseme, I.M. Uriri, R. Hawkins, R.G. Rank, Integrin-mediated epithelial–T cell interaction enhances nitric oxide production and increased intracellular inhibition of Chlamydia, J. Leukoc. Biol. 59 (1996) 656–662.
[33] S. Kwon, S.C. George, Synergistic cytokine-induced nitric oxide production in human alveolar epithelial cells, Nitric Oxide 3 (1999) 348–357.
[34] S. Bulfone Paus, E. Bulanova, T. Pohl, V. Budagian, H. Durkop, R. Ruckert, U. Kunzendorf, R. Paus, H. Krause, Death deflected: IL-15 inhibits TNF-α-mediated apoptosis in fibroblasts by TRAF2 recruitment to the IL-15Rα chain, FASEB J. 13 (1999) 1575–1585.
[35] G.J. Della Rocca, S. Maudsley, Y. Daaka, R.J. Lefkowitz, L.M. Luttrell, Pleiotropic coupling of G protein-coupled receptors to the mitogen-activated protein kinase cascade. Role of focal adhesions and receptor tyrosine kinases, J. Biol. Chem. 274 (1999) 13978–13984.
[36] N. Niisato, Y. Marunaka, Blocking action of cytochalasin D on protein kinase A stimulation of a stretch-activated cation channel in renal epithelial A6 cells, Biochem. Pharmacol. 61 (2001) 761–765.
[37] P. Estess, A. Nandi, M. Mohamadzadeh, M.H. Siegelman, Interleukin 15 induces endothelial hyaluronan expression in vitro and promotes activated T cell extravasation through a CD44-dependent pathway in vivo, J. Exp. Med. 190 (1999) 9–19.
[38] M. Li, L. Rosenfeld, R.E. Vilar, M.K. Cowman, Degradation of hyaluronan by peroxynitrite, Arch. Biochem. Biophys. 341 (1997) 245–250.

# A Nontoxic Chimeric Enterotoxin Adjuvant Induces Protective Immunity in Both Mucosal and Systemic Compartments with Reduced IgE Antibodies

Mi-Na Kweon,[1,a] Masafumi Yamamoto,[1,2,a] Fumiko Watanabe,[3] Shinichi Tamura,[4] Frederik W. van Ginkel,[7] Akira Miyauchi,[3] Hiroaki Takagi,[3] Yoshifumi Takeda,[4] Takashi Hamabata,[5] Kohtaro Fujihashi,[7] Jerry R. McGhee,[7] and Hiroshi Kiyono[1,6,7]

[1]*Department of Mucosal Immunology, Research Institute for Microbial Diseases, Osaka University, Osaka,* [2]*Department of Oral Medicine, Nihon University School of Dentistry at Matsudo, and* [3]*Protein Express and Higeta Shoyu, Chiba, and* [4]*National Institute of Infectious Diseases,* [5]*International Medical Center of Japan, and* [6]*Division of Mucosal Immunology, Institute of Medical Science, University of Tokyo, Tokyo, Japan;* [7]*Immunobiology Vaccine Center, Departments of Microbiology and of Oral Biology, University of Alabama at Birmingham, Birmingham*

**A novel nontoxic form of chimeric mucosal adjuvant that combines the A subunit of mutant cholera toxin E112K with the pentameric B subunit of heat-labile enterotoxin from enterotoxigenic *Escherichia coli* was constructed by use of the *Brevibacillus choshinensis* expression system (mCTA/LTB). Nasal immunization of mice with tetanus toxoid (TT) plus mCTA/LTB elicited significant TT-specific immunoglobulin A responses in mucosal compartments and induced high serum immunoglobulin G and immunoglobulin A anti-TT antibody responses. Although TT plus native CT induced high total and TT-specific immunoglobulin E responses, use of the chimera molecule as mucosal adjuvant did not. Furthermore, all mice immunized with TT plus mCTA/LTB were protected from lethal systemic challenge with tetanus toxin. Importantly, the mice were completely protected from influenza virus infection after nasal immunization with inactivated influenza vaccine together with mCTA/LTB. These results show that *B. choshinensis*–derived mCTA/LTB is an effective and safe mucosal adjuvant for the induction of protective immunity against potent bacterial exotoxin and influenza virus infection.**

An important feature of immune responses at mucosal surfaces is the production of secretory IgA antibodies and their transport across the epithelium. This immune response represents the first line of defense against invasion by viral and bacterial pathogens [1]. Therefore, recent efforts have been focused on the development of vaccines capable of inducing effective immune responses in mucosal tissues; however, most protein antigens are rather weak immunogens when given via a mucosal route. Thus, the development of effective and reliable mucosal adjuvants that can be safely coadministered with vaccine antigen is of central importance for new-generation vaccines.

Cholera toxin (CT) produced by *Vibrio cholerae* is structurally similar to the heat-labile enterotoxin (LT) of enterotoxigenic *Escherichia coli*, and both toxins act as adjuvants for enhancement of mucosal and serum antibody responses to coadministered protein antigens given by either oral or nasal routes [2]. Despite the potent mucosal adjuvant activity of native (n) CT and nLT, both enterotoxins cause severe diarrhea and thus are unsuitable for use in humans [3]. Therefore, a number of nontoxic mutant (m) derivatives of CT or LT have been constructed [4–10]. We also have generated mCT by substituting a single amino acid in the ADP-ribosyltransferase active center of the A subunit and have created 2 mutants of CT (S61F and E112K) [11]. These newly created forms of mCT did not induce ADP-ribosylation and cAMP formation but still served as a mucosal adjuvant by inducing $CD4^+$ Th2-type cells. Those cells, in turn, provided effective help for antigen-specific mucosal secretory IgA, as well as serum IgG and IgA antibody responses [12–14]. Furthermore, antigen-specific mucosal IgA and serum IgG antibody responses induced by mCT were protective against challenge with bacterial or viral pathogens [12, 14, 15].

In this study, we have constructed a novel chimeric adjuvant that combines the A subunit of mCT E112K and the B subunit of LT (mCTA/LTB) in a *Brevibacillus choshinensis* host–vector system. We also further assessed mucosal adjuvant properties, as well as the usefulness of *B. choshinensis*–generated mCTA/LTB for the induction of protective immunity.

Received 17 April 2002; revised 5 June 2002; electronically published 3 October 2002.

Financial support: Ministry of Heath, Labor, and Welfare of Japan; Ministry of Education, Culture, Sports, Science, and Technology; Japan Society for the Promotion of Science (Grant-in-Aid for Encouragement of Young Scientists); Japan Health Sciences Foundation; National Institutes of Health (grants AI-35932, DE-09837, AI-43197, AI-18958, DK-44240, AI-43197, DE-12242, DC-04976, and AI-65299).

[a] M.-N.K. and M.Y. contributed equally to this work.

Reprints or correspondence: Dr. Hiroshi Kiyono, Dept. of Mucosal Immunology, Research Institute for Microbial Diseases, Osaka University, Osaka 565-0871, Japan (kiyono@biken.osaka-u.ac.jp).

**The Journal of Infectious Diseases 2002;186:1261–9**
© 2002 by the Infectious Diseases Society of America. All rights reserved.
0022-1899/2002/18609-0008$15.00

## Materials and Methods

*Plasmid construction.* A plasmid containing both *mCTA* E112K and *LTB* genes was constructed as follows. First, the *mCTA* gene was amplified by use of polymerase chain reaction (PCR), using pUC119-E112K as a template and the following primer set: mCTA-M (5′-AACCATGGCTTTCGCTAATGATGATAAGTTATAT-3′) and mCTA-R (5′-TTAAGCTTCATAATTCATCCTTAATTCT-3′) [11]. The PCR product was digested with *Nco*I and *Hin*dIII and then was inserted to pNCMO2 digested with the same enzymes to give pNCMO2-mCTA. Second, the *LTB* gene also was amplified by use of PCR with the following primer set (LTB-M, 5′-AACCATGGCTTTCGCTGCTCCCCAGACTATTACAGA-3′; LTB-R, 5′-AAGGATCCCTAGTTTTTCATACTGATTGC-3′) from the chromosome of enterotoxigenic *E. coli* WT-1 [16]. The PCR product was cloned into the *Nco*I/*Bam*HI site of pNCMO2 after digestion with *Nco*I and *Bam*HI to give pNCMO2-LTB. Third, the mCTA gene together with the preceding ribosome binding site (SD2) of *B. choshinensis* cell wall protein gene was amplified with BAMSD primer (5′-AAAGGATCCTAGAGGAGGAGAACACAAGG-3′) and mCTA-R primer from pNCMO2-mCTA [17]. The amplified SD2-mCTA gene was digested with *Bam*HI and *Hin*dIII and then was cloned into the *Bam*HI/*Hin*dIII site of pNCMO2-LTB, resulting in pNCMO2-LTB-mCTA (figure 1*A*). The expression plasmid, pNCMO2-LTB-mCTA, was introduced into *B. choshinensis* by use of electroporation, as described elsewhere [18].

*Production and purification of mCTA/LTB chimera.* The *E. coli* JM109 strain (TaKaRa Shuzo) was used as cloning host, and *B. choshinensis* HPD31 was used as host for production of the recombinant protein [19]. The *E. coli–B. choshinensis* expression-secretion shuttle vector pNCMO2 was constructed by inserting the pUC119-derived *ColE1* replication origin and ampicillin resistance gene (TaKaRa Shuzo) into pNH301 [20]. Additionally, the *lac* operator derived from pUC119 was inserted in front of a promoter 2 region, as described elsewhere [17]. For cultivation, 2SLN medium and LB broth were used for the *B. choshinensis*–harboring plasmid and *E. coli*, respectively. The transformation containing pNCMO2-LTB-mCTA was cultured in 2SLN medium for 3 days at 30°C. After cultivation, the mCTA/LTB chimera protein in the culture supernatant was purified by fractionation on an immobilized D-galactose column (Pierce Chemicals), according to the method described elsewhere [21]. The culture supernatant was applied to the column and then was eluted with 0.2 *M* galactose in 50 m*M* phosphate buffer (pH 8.0). The extract then was filtered by use of a 30,000-molecular-weight ultrafiltration membrane (Biomax-30; Millipore) to remove endotoxin. The filtrate was concentrated and dialyzed against pyrogen-free 20 m*M* phosphate buffer (pH 8.0) by use of a 5000-molecular-weight ultrafiltration membrane (Biomax-5; Millipore). The purity of the molecules was examined by SDS-PAGE. The protein concentration was determined by use of MicroBCA protein assay reagent (Pierce).

*Bioassay and toxicity of mCTA/LTB.* The ability of mCTA/LTB and nCT (List Biological Laboratories) to induce toxic effects on cultured Chinese hamster ovary (CHO) cells was investigated, as described elsewhere [11]. The toxicity of each adjuvant was determined as the induction of spindle formation in >20% of cultured CHO cells. For the cAMP assay, $10^5$ CHO cells in MEM alpha medium containing 1% fetal calf serum were cultured with 1 ng/mL of nCT or mCTA/LTB at 37°C in a 5% $CO_2$ incubator for 24 h. Intracellular cAMP was measured by use of an EIA kit (Amersham). The endotoxin levels were determined by use of the Limulus J test (Wako), and in vitro toxicity was examined by use of a mouse ileal loop test [22]. In brief, mice were anesthetized, and 100 μL of PBS containing different doses of mCTA/LTB or nCT was injected into 2-cm sutured ileal loops. The mice were killed 18 h later, and the ratio of fluid to length was defined as being positive when the ratio was >40 μL/cm.

*Trafficking of radiolabeled protein vaccine and adjuvants.* Tetanus toxoid (TT) and mCTA/LTB were radiolabeled with $^{125}$I, as described elsewhere [23]. To assess the redirection ability of vaccine antigen by mCTA/LTB, mice were given $^{125}$I-conjugated TT together with nCT or mCTA/LTB via the nasal route. Uptake of $^{125}$I-labeled TT into neuronal and lymphoid tissues was assessed over a 6-day period. In addition, $^{125}$I-conjugated mCTA/LTB was given nasally to address their presence in central nervous system tissues at 6, 12, 24, 72, and 144 h. The counts per minute present in the different tissues were determined by use of a gamma counter. The microBCA protein assay was used to determine the protein concentrations of radiolabeled proteins. This allowed for the calculation of the specific activity of $^{125}$I-labeled TT (87 cpm/ng) and $^{125}$I-conjugated mCTA/LTB (1605 cpm/ng), for the determination of the amount of protein associated with the different organs. A total of 6.8 μg of $^{125}$I-labeled TT was applied nasally with the mucosal adjuvants nCT (1.0 μg) or mCTA/LTB (2.5 μg) for antigen redirection studies, and a total of 2.0 μg of $^{125}$I-conjugated mCTA/LTB was used for the neuronal targeting studies. All nasal applications were given in a final volume of 10–12 μL, that is, 5–6 μL per nares, to naive mice. About 43% of the $^{125}$I-conjugated mCTA/LTB bound to ganglioside GM1.

*Mice and immunization protocols.* Female C57BL/6 mice aged 5–6 weeks were purchased from Japan Clea and were housed in the experimental animal facility at the Research Institute for Microbial Diseases (Osaka University). Mice were immunized nasally on days 0, 7, and 14 with a 20-μL aliquot (10 μL/nostril) of PBS containing 5 μg of TT (provided by Dr. Yasushi Higashi, Osaka University, Biken Foundation, Osaka, Japan) alone or combined with 0.5 μg of nCT or 10 μg of mCTA/LTB. In the influenza virus studies, female BALB/c mice (SLC) were used in all experiments. Hemagglutinin (HA) vaccines (split-product virus vaccines) were prepared from influenza virus A/PR/8/34 (PR8, H1N1) by the method of Davenport et al. [24]. Mouse-adapted PR8 virus was passaged 148 times in the ferret, 596 times in the mouse, and 73 times in 10-day fertile chicken eggs. Mice were anesthetized and then were immunized nasally by dropping PBS containing mCTA/LTB chimera (5 μg/2 μL) plus HA vaccine (5 μg/2 μL) into each nostril [25]. Four weeks later, these mice were boosted with an identical immunization regimen.

*Sample collection.* Saliva, nasal wash, and serum samples were collected to examine TT- or HA-specific antibody responses. Saliva samples were obtained from mice after intraperitoneal injection with 100 μg of sterile pilocarpine [14]. Nasal wash specimens were collected by gently flushing the nasal passages with 100 μL of sterile PBS [14]. Alternatively, a hypodermic needle was inserted into the posterior opening of the nasopharynx, and 1 mL of PBS containing 0.1% bovine serum albumin was injected 3 times [26]. To obtain lung washes, the trachea and lungs were taken out and the washing

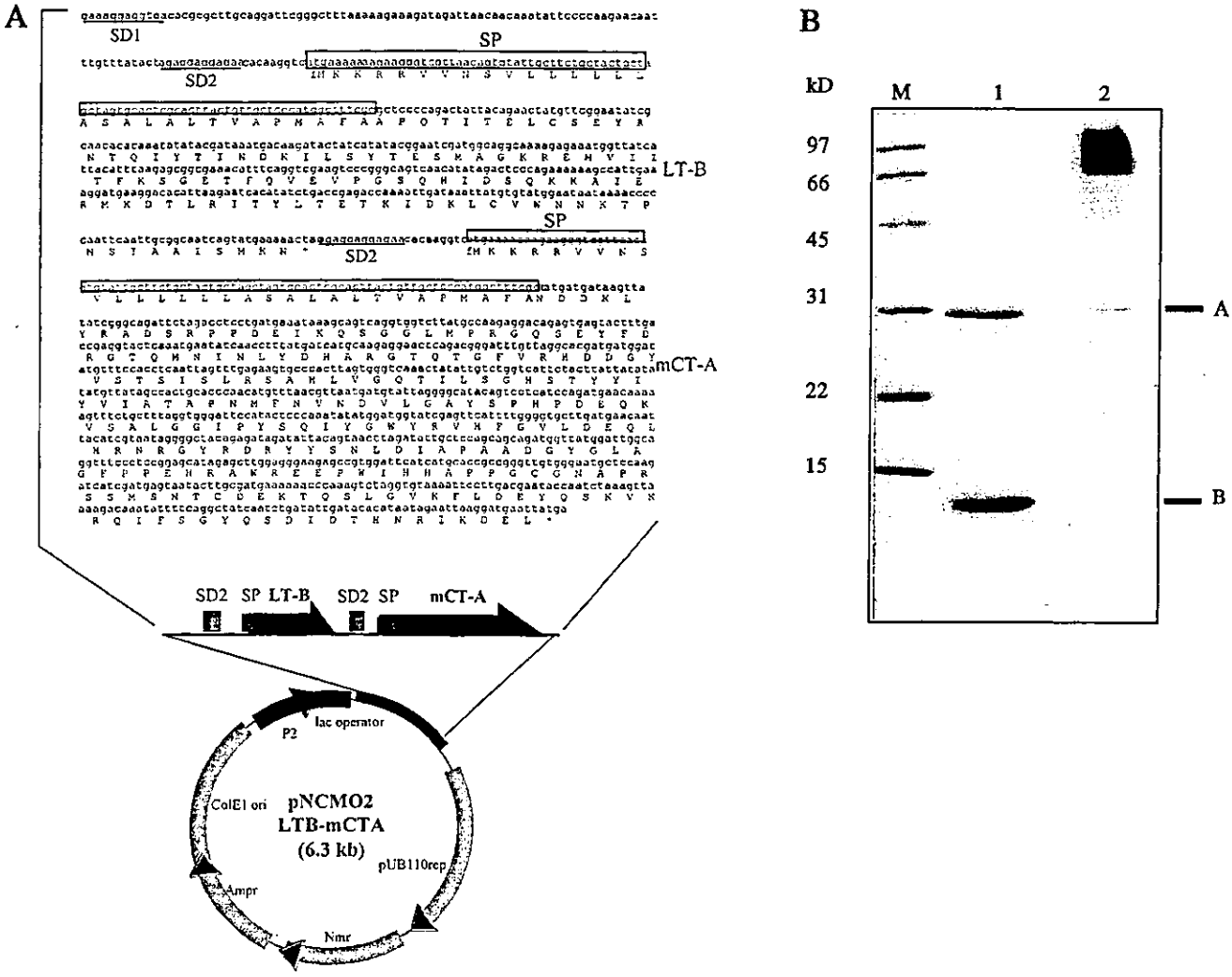


**Figure 1.** Development of chimeric mucosal adjuvant that combines A subunit of mutant cholera toxin E112K with pentameric B subunit of heat-labile enterotoxin from enterotoxigenic *Escherichia coli* (mCTA/LTB). *A,* Structure of mCTA/LTB chimera expression-secretion shuttle vector pNCMO2-LTB-mCTA. Sequences encoding mature mCTA and LTB genes are directly fused to signal sequence. *B,* SDS-PAGE analysis of purified mCTA/LTB chimera. Proteins were stained with Coomassie brilliant blue. Samples were loaded onto 15% SDS-polyacrylamide gels under reducing *(lane 1)* or nonreducing *(lane 2)* conditions. Molecular mass markers (M) are at left. A, mCTA subunit; *Ampr,* ampicillin resistance gene; B, LTB subunit; SD1, SD2, ribosome-binding sites; SP, signal peptide–encoding sequence; P2, promoter 2 region of cell wall protein gene of *Brevibacillus choshinensis;* pUB110rep, pUB110 origin of replication.

process was done twice with 2 mL of PBS containing 0.1% bovine serum albumin, as described elsewhere [26].

*Antigen-specific antibody titers by ELISA.* Antigen-specific antibody titers in serum and mucosal secretions were determined by ELISA, as described elsewhere [25, 27]. To quantify the level of PR8 HA-specific antibodies, polyclonal PR8 HA-specific IgA and IgG antibodies were affinity-purified from the lung washes of mice immunized nasally with adjuvant (e.g., nCT)–combined PR8 HA molecules [25]. Affinity-purified IgG and IgA antibodies (100 ng/mL) were routinely used as a standard [25]. The antibody concentration of an unknown specimen was determined from the standard regression curve constructed for each assay.

*ELISA for total and TT-specific IgE antibodies in serum.* For detection of total and TT-specific serum IgE antibody levels, 96-well plates (Nunc) were coated with rat anti–mouse IgE monoclonal antibody (R35-72; BD PharMingen) [28]. After blocking, serial dilutions of serum samples were made, and standard mouse IgE (27-74l; BD PharMingen) was added. After incubation, biotinylated rat anti–mouse IgE monoclonal antibody (R35-118; BD PharMingen) for determining total IgE levels or biotinylated TT for determining TT-specific IgE antibodies was added, followed by horseradish peroxidase–labeled anti-biotin monoclonal antibody (Vector Laboratories). Endpoint titers of TT-specific IgE were expressed as reciprocal $\log_2$ titers.

*Tetanus toxin challenge.* Tetanus toxin for the challenge experiments was provided by Dr. Yasushi Higashi. The toxin was

diluted in 0.5% gelatin/PBS, and the appropriate minimum lethal dose (130 $LD_{50}$) was given subcutaneously to each mouse group. The mice were monitored daily for paralysis and death [27].

*Influenza virus infection.* Two weeks after the last nasal immunization, the mice were infected nasally by dropping 20 μL of PBS containing a PR8 virus suspension with $10^{4.1}$ $EID_{50}$ per mouse [29]. This procedure induced a total respiratory tract infection that caused virus shedding from nose and lung and led to viral pneumonia and death ~7 days after infection. Lung wash on day 3 after infection was collected, and 200-μL aliquots of each serial 10-fold dilution were injected into Madin-Darby canine kidney cells in a 6-well plate. After 1 h of absorption, each well in the plate was overlaid with 2 mL of agar medium, according to methods described elsewhere [30, 31]. The plaques were developed for 2 day during incubation in a $CO_2$ incubator and then were counted. The virus titer was expressed as plaque-forming units per milliliter.

*Data and statistical analysis.* Data were expressed as mean ± SE and were evaluated by use of the Mann-Whitney *U* test for unpaired samples, using a Statview II statistical program designed for the Macintosh computer. $P < .05$ was considered to be statistically significant.

## Results

*Properties of mCTA/LTB chimera constructed with* B. choshinensis *HPD31.* A plasmid consisting of LTB and mCTA E112K was constructed by using the pNCMO2 shuttle vector system (figure 1*A*). A large amount of mCTA/LTB chimera protein (2 mg/L) was secreted by *B. choshinensis* harboring pNCMO2-LTB-mCTA, and SDS-PAGE revealed it to have 2 bands, corresponding to mCTA and LTB (figure 1*B*). The ratio of the amounts of these 2 components was ~1:5, which suggests that each component combined to form 1 molecule of mCTA with the pentameric LTB complex. This assumption was supported further by SDS-PAGE analysis of the chimeric protein together with nLT carried out under nonreducing and denaturing conditions. Both proteins migrated to identical positions in the gel (data not shown).

*The mCTA/LTB chimera is nontoxic and enzymatically inactive.* The biologic properties and toxicity of mCTA/LTB were examined and were compared with those of nCT (table 1). Although 1 ng of nCT induced extensive spindle cell formation in CHO cells, mCTA/LTB chimera, at doses as high as 1 μg, did not. Furthermore, CHO cells treated with mCTA/LTB did not produce cAMP. We confirmed that the mCTA/LTB chimera was nontoxic by use of mouse ileal loop test. Although 100 ng of nCT induced significant fluid accumulation, a 1000-fold–higher level of mCTA/LTB did not induce any detectable fluid accumulation (table 1).

*Influence of nasal mCTA/LTB on trafficking of coadministered vaccine.* To determine whether mCTA/LTB redirects vaccine protein, $^{125}$I-labeled TT distribution in various tissues was analyzed after nasal administration with mCTA/LTB plus $^{125}$I-labeled TT and was compared with groups inoculated with $^{125}$I-labeled TT given alone or together with nCT (figure 2*A*). Interestingly, lower levels of $^{125}$I-labeled TT accumulation were observed in the olfactory nerves and epithelium isolated from the group given $^{125}$I-labeled TT plus mCTA/LTB nasally than from the group given $^{125}$I-labeled TT plus nCT. In contrast, no significant difference was seen in several lymphoid tissues, the olfactory bulbs, or brain of mouse groups given nasal $^{125}$I-labeled TT plus mCTA/LTB or nCT or $^{125}$I-labeled TT alone. In the next study, $^{125}$I-conjugated mCTA/LTB alone was given nasally, and neuronal tissues (olfactory bulbs, olfactory nerves and epithelium, and brain) were analyzed for the presence of $^{125}$I-conjugated mCTA/LTB (figure 2*B*). In contrast to the $^{125}$I-labeled TT redirection experiments, the $^{125}$I-conjugated mCTA/LTB itself was present in the olfactory nerves and epithelium and peaked at 6 h, plateaued, and remained detectable for 6 days. In addition, $^{125}$I-conjugated mCTA/LTB in the olfactory bulbs peaked at 12 h and remained relatively constant over 6 days. We have reported that an accumulation of 1–2 ng of nCT was seen routinely in the olfactory bulbs during the 6 days when these tissues were analyzed after 10 μg of nCT was given nasally [23]. There was an ~2-fold–higher accumulation in the olfactory bulbs (3–4 ng) with the chimeric mCTA/LTB compound when 2.0 μg was given nasally (figure 2*B*). On the other hand, the targeting levels of mCTA/LTB were similar or even lower in the olfactory nerves and epithelium and in brain after 2.0 μg of $^{125}$I-conjugated mCTA/LTB was given, compared with that of $^{125}$I-labeled nCT administered nasally [23] (figure 2*B*). Overall, although nasal administration of mCTA/LTB targeted neuronal tissues, it did not affect trafficking of coadministered vaccine antigens into the neuronal tissues.

*The mCTA/LTB chimera adjuvant supports TT-specific mucosal secretory IgA and serum IgG antibody responses.* To assess the mucosal adjuvant properties of mCTA/LTB, mice were immunized nasally with TT plus mCTA/LTB. Nasal immunization with TT plus mCTA/LTB resulted in significant TT-

**Table 1.** Biologic characteristics and potential toxicity of chimeric mucosal adjuvant that combines A subunit of mutant cholera toxin E112K with pentameric B subunit of heat-labile enterotoxin from enterotoxigenic *Escherichia coli* (mCTA/LTB).

| Adjuvant | CHO assay, ng of protein[a] | cAMP induction, pmol[b] | Ileal loop test, ng of protein[c] |
|---|---|---|---|
| nCT | 1.0 | 3.92 ± 0.01 | 100 |
| mCTA/LTB | >$10^3$ | 0 | >$10^3$ |

NOTE. CHO, Chinese hamster ovary; nCT, native cholera toxin.

[a] CHO cells were cultured in MEM alpha medium containing 1% FBS with $\log_{10}$ dilutions of each adjuvant for 24 h and the toxic effect were determined as spindled formation in >20% of cultured cells.

[b] CHO cells ($1 \times 10^5$ cells/well) were cultured in medium containing 1% FBS with 1 ng/mL of each adjuvant for 24 h, and the cAMP induction were assessed using ELISA.

[c] Enterotoxicity of each adjuvant were measured by use of ileal loop test, where 100 μL of PBS containing different levels of each adjuvant were injected into 2 cm ileal loop of anesthetized mice. The amount of fluid to length were measured 18 h later and were defined as positive when the ratio was >40 μL/cm.

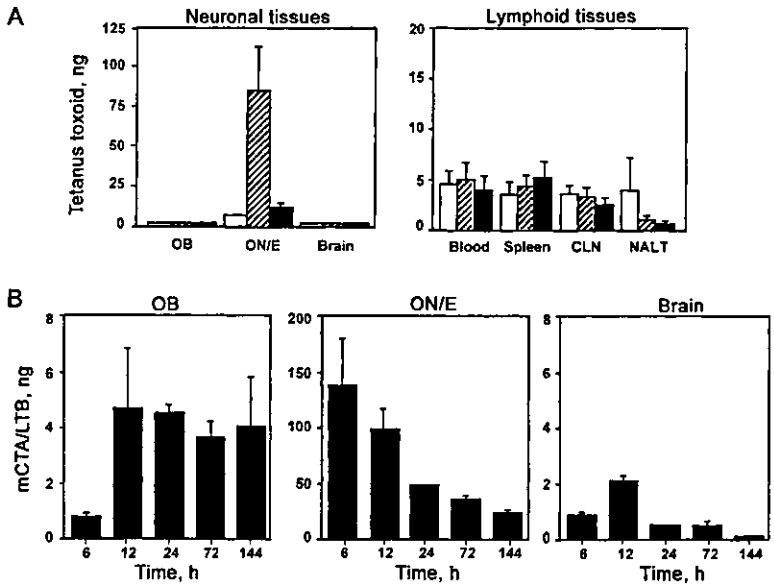


Figure 2. Trafficking effects of the chimeric adjuvant. *A,* Trafficking of radiolabeled vaccine antigen (tetanus toxoid [TT]) in lymphoid and neuronal tissues 6 days after nasal challenge with *(hatched bars)* or without *(open bars)* native cholera toxin (CT) or chimeric adjuvant that combines A subunit of mutant CT with pentameric B subunit of heat-labile enterotoxin from enterotoxigenic *Escherichia coli* (mCTA/LTB; *solid bars*). *B,* Distribution of radiolabeled mCTA/LTB in olfactory nerves and epithelium (ON/E), olfactory bulbs (OB), and brain after nasal challenge with $^{125}$I-conjugated mCTA/LTB alone. Specific activities: $^{125}$I-labeled TT, 87 cpm/ng; $^{125}$I-conjugated mCTA/LTB, 1605 cpm/ng.

specific serum IgG and IgA antibody responses, compared with those induced by TT together with nCT (figure 3*A*). In particular, the profiles of serum IgG1 and IgG2a antibody responses of mice given TT plus mCTA/LTB nasally were similar to those of mice given TT together with nCT (figure 3*A*). On the other hand, nasal administration of nCT or mCTA/LTB alone failed to elicit TT-specific antibody responses in the starting dilution ($\log_2$ of 6) used in these experiments (data not shown). In addition, nasal administration of TT plus mCTA/LTB chimera induced high levels of TT-specific IgA antibody responses in saliva, as well as nasal wash samples, compared with those induced by TT plus nCT (figure 3*A*).

To determine whether IgA antibody responses in external secretions were mucosa-associated or, alternatively, were exudates from serum, the numbers of antigen-specific IgA antibody–forming cells were measured. High numbers of TT-specific IgA antibody–forming cells were found in the submandibular gland and nasal passages of mice given TT plus mCTA/LTB or nCT, whereas low numbers of antibody-forming cells were detected in the submandibular gland and nasal passages of mice given TT alone (data not shown). These findings demonstrate that a new chimeric molecule of mCTA/LTB is a potent mucosal adjuvant for the induction of vaccine antigen–specific mucosal IgA and systemic IgG antibody responses.

*Induction of neutralizing antibody responses to tetanus toxin by nasal immunization.* Because nasal TT plus mCTA/LTB elicited high levels of antigen-specific IgG and IgA antibody responses, we determined if these antibodies also were protective. Mice given TT plus mCTA/LTB chimera or nCT as mucosal adjuvant, or TT alone, were challenged with a lethal dose (130 $LD_{50}$) of tetanus toxin and were monitored for paralysis and death. As expected, nasal immunization with TT plus nCT provided complete protection (figure 3*B*). Of importance, equal protection was provided when TT was given with mCTA/LTB and when nCT was used as a mucosal adjuvant. In contrast, TT, mCTA/LTB, or nCT alone provided no protection for mice against the paralysis and death that normally occurs within 1 day after administration of tetanus toxin (figure 3*B*). These findings clearly demonstrate the effectiveness of mucosally induced serum TT-specific IgG antibodies by coadministered mCTA/LTB chimera as mucosal adjuvant.

*Lack of induction of IgE antibody responses by mCTA/LTB chimera.* To determine whether the newly constructed *B. choshinensis*–derived chimeric mCTA/LTB enhanced IgE antibody responses, we measured both total and TT-specific IgE antibody titers in serum samples of mice immunized nasally with TT plus mCTA/LTB or nCT. As might be expected, high levels of total and TT-specific IgE antibody responses were induced in serum of mice given TT plus nCT (figure 4). Interestingly, however, significantly lower levels of total and TT-specific IgE antibodies were noted in mice given nasal TT plus mCTA/LTB than in mice immunized with TT plus nCT (figure 4). It is possible that mCTA/LTB or mCT E112K may lead to different kinetics for TT-specific IgE antibody responses. There-